SEA
GRANT
PROJECT
OFFICE

ENGINEERING ASPECTS OF FRACTURE TOUGHNESS: FIBER REINFORCED LAMINATES

by

John F. Mandell
Frederick J. McGarry
Reiichiro Kashihara
William O. Bishop

Massachusetts Institute of Technology
Cambridge, Massachusetts 02139

Report No. MITSG 73-9
June 30, 1973

ENGINEERING ASPECTS OF FRACTURE TOUGHNESS: FIBER REINFORCED LAMINATES

by

John F. Mandell
Frederick J. McGarry
Reiichiro Kashihara
William O. Bishop

Report No. MITSG 73-9
Index No. 73-309-Cfo

ABSTRACT

The results of an experimental investigation into the variables which affect the fracture toughness of several common varieties of fiber reinforced plastics are discussed. The fundamental mechanism by which composites of the type investigated resist crack extension is by the growth of subcracks which blunt the main crack tip and reduce the concentration of stress. This mechanism results in an inherently blunt crack tip which may preclude the meaningful application of classical linear elastic fracture mechanics; an alternative fracture criterion based upon a more acceptable generalized stress concentration concept is suggested. The fracture toughness is found to increase with decreasing temperature and increasing strain rate, but is insensitive to laminate thickness in many cases. While the laminate fracture toughness is strongly influenced by fiber orientation, fiber volume fraction, and ply stacking arrangement, the properties of the matrix material have little effect.

INTRODUCTION

Numerous investigators have studied the fracture resistance of fiber reinforced plastics in recent years, particularly from the viewpoint of the applicability of linear elastic fracture mechanics (LEFM). Results of tests on a variety of laminate types, such as those given by Owen and Bishop [1], indicate that the fracture behavior may or may not be consistent with the basic concepts of LEFM theory, depending upon the style of reinforcement used. The extreme examples of behavior are observed for unidirectional composites, where a crack introduced parallel to the fibers will propagate colinearly with the original crack, in a brittle fashion consistent with the assumptions of LEFM [2], while a crack introduced normal to the fibers will usually deflect and propagate parallel to the fibers, contrary to the assumptions of LEFM [3].

Previous studies [4,5,6] have shown that the initial response of a laminate to a load in the presence of a sharp stress concentration is the propagation of subcracks parallel to the local fiber direction at any point. For practical composites such as the crossplied, woven fabric, or chopped fiber mat styles, this results in numerous subcracks extending in several directions at the tip of a main, through-thickness notch. These subcracks, which also accompany main crack extension, apparently serve to blunt the main crack tip as originally envisioned by Cook

and Gordon [7]. The length of subcrack extension has been related directly to the fracture toughness of the laminate [4,5].

Although progress has been made in characterizing the applicability of LEFM and in understanding the origins of the toughness, few data are available to characterize effects such as thickness, strain rate, and temperature which have been major considerations in brittle service failures of homogeneous materials. In addition to continuing the investigation of fracture criteria, origins of toughness, and variations in material characteristics such as fiber orientation, the work reported in this paper also considers the influence of these other variables.

MATERIALS AND TEST METHODS

The following are the principal materials investigated in this study:

1. Scotchply Type 1002 unidirectional-ply E-glass/epoxy (3M Co.) in various ply configurations.
2. Laminac 4155 polyester matrix with MEK peroxide catalyst (American Cyanamid Co.) reinforced with 18 oz/yd^2 E-glass woven-roving Style 779 (J.P. Stevens Fiberglass Co.) and Style 61 (Uniglass Industries), and 1.5 oz/ft^2 random chopped fiber mat using approximately two inch E-glass strands (Ferro Corp.), or combinations thereof.

3. Laminac 4173 polyester matrix with MEK peroxide catalyst (American Cyanamid Co.) reinforced with 8.9 oz/yd^2 Style 181 E-glass woven fabric (J.P. Stevens Fiberglass Co.).

Material (1) was compression molded in accordance with manufacturer's instructions; Materials (2) were fabricated by hand lay-up, and Material (3) was compression molded using a vacuum bag. The fiber volume fraction for each material tested is given in Table 1 while the fiber orientation will be given later for each case.

The laminates were machined to the specimen shapes indicated in Figure 1 using a diamond-edged wheel and a TensilKut router; notches were cut with a thin diamond-edged wheel. The particular shape of the unnotched tensile specimen was determined by trial and error to give the highest stress at failure without breaking in the grips; despite these efforts, fractures originated in some cases in the transition region rather than in the gage section.

The value of the critical stress intensity factor, K_Q, was determined from available K-calibrations for isotropic materials.* For the DEN specimen K_Q is

---

*The subscript Q used with K_Q indicates the candidate opening mode critical stress intensity factor as suggested by ASTM [8]; the candidate value is distinct from K_{Ic} as the latter satisfies certain validity requirements which are not available yet for composites.

determined from [9] as:

$$K_Q = \sigma_f Y \sqrt{c} \tag{1}$$

where σ_f is the applied stress at fracture and Y is given by:

$$Y = 1.98 + 0.36\left(\frac{2c}{w}\right) - 2.12\left(\frac{2c}{w}\right)^2 + 3.42\left(\frac{2c}{w}\right)^3$$

For the cleavage specimen K_Q is given in [10] as:

$$K_Q = \frac{P_f}{tH^{1/2}}\left(\frac{c}{H} + 0.7\right) \tag{2}$$

where P_f is the applied load at fracture, t is the thickness and H is the half-width; for the specimen shown in Figure 1, Equation (2) reduces to:

$$K_Q = P_f(8.72c + 9.13)$$

where P_f is the applied load at fracture. Although the K-calibration for the cleavage specimen assumes infinite length, it is in good agreement with the finite element data given by Kanninen [11] for this specimen size in crack lengths of practical interest. Unpublished finite element and experimental results which consider the effects of anisotropy indicate a maximum deviation from the isotropic K-calibrations of approximately ten percent.

The critical strain energy release rate (fracture work or energy), G_Q, can be measured directly for the cleavage specimen as described in Reference [4]. Assuming the validity of LEFM, G_Q is related to K_Q for an orthotropic material with coincident structural and material principal directions by [12]:

$$G_Q = K_Q^2 \left[\frac{A_{11}A_{22}}{2}\right]^{1/2} \left[\left(\frac{A_{22}}{A_{11}}\right)^{1/2} + \frac{2A_{12}+A_{66}}{2A_{11}}\right]^{1/2} \quad (3)$$

where the A_{ij} terms are from the stress-strain relations

$$[\varepsilon] = [A][\sigma]$$

The procedure for measuring the fracture toughness was to load the specimen until fracture occurred, noting the maximum load. In most cases the load-deflection curve was approximately linear to fracture, so the load used in calculating K_Q was clearly defined as the maximum load. Fracture of the cleavage specimen proceeded in a stable fashion down the length of the specimen, with an increasing deflection necessary to keep the crack moving; the load to cause initial crack extension from the precut notch was used in calculating K_Q for this case. An Instron universal testing machine was used for all tests, with a displacement rate of 0.05 inches/minute and laboratory temperature and humidity unless otherwise noted. The replication factor for most experiments was three, with a minimum of two in some cases. All results are calculated using an average ply thickness for all specimens of a given series; thicknesses for each material are given in Table 1.

CHARACTERISTICS OF FRACTURE

The characteristics of crack propagation in crossplied, woven fabric, and chopped fiber mat reinforced polyester and epoxy have been described previously for glass and

graphite fiber reinforcement [4,5,6]. When a crack propagates so as to cause failure of the fibers in at least one direction, the growth of subcracks parallel to the fibers results in a ligamented appearance of the fracture region, with the typical subcracks extending a tenth of an inch on both sides of the main fracture plane. Figure 2 indicates the ligamented appearance of the fracture region for a crack growing normal to the unidirectional 0° fibers of a 0°/90° crossplied E-glass/epoxy laminate; the crack tip is blunted by the split parallel to the fibers.

The blunting of the main crack is even more distinct in the case of a partial through-thickness crack, as shown in Figures 3 and 4. In this case the crack was introduced into the Scotchply laminate during fabrication by cutting the prepreg tape with a razor blade. During cure of the laminate the cut filled with epoxy, which, upon loading of the specimen, fractured at a low stress level, forming a sharp surface crack. At higher stress levels the usual subcracks formed in the cut 0° and 90° plies and a zone of delamination formed between the last cut ply and the first uncut ply (Figure 4a). Crack extension occurred by growth of the crack in the cut plies, in the manner indicated in Figure 2, with the delamination zone simultaneously spreading over a large area as shown in Figure 4b. Finally the cut plies may separate completely from the uncut plies before total failure of the laminate.

Fracture of a laminate containing a surface crack is different from fracture of a homogeneous material in which the crack propagates through the specimen to form a through-thickness crack. The role of delamination between plies is clearly evident in Figure 3; delamination may also play an important role in the fracture of certain angle-plied laminates containing a through-thickness crack. As shown in Figure 5, taken from Reference [6], fracture may occur by the propagation of a delamination zone accompanied by buckling of the fibers which cross the zone, with the major deformation being shear parallel to the crack rather than opening of the crack. In this case the interlaminar strength and toughness, rather than the fiber strength, will determine the fracture resistance.

Almost without exception the fracture characteristics of woven fabric, woven roving and chopped fiber mat reinforced composites is in the opening mode, displaying the ligamented fracture region shown in Figure 2 [4,5]. Since such a material may contain randomly oriented strands, and warp and fill yarns of various size and direction, the growth of subcracks and yarn debonding zones [4] at the main crack tip are very complex and difficult to delineate. Figure 6 shows a stationary crack in such a laminate, consisting of woven roving and chopped mat.

NOTCH GEOMETRY EFFECTS

Experience with metals which fail by brittle fracture indicates that the dominant features of a notch are its length and tip radius [13]. In an otherwise uniform stress field in a large specimen, the introduction of an elliptical notch produces a maximum stress at the notch tip of [14]:

$$\sigma_{max} = \sigma(1 + 2\sqrt{c/\rho}) \tag{4}$$

where ρ is the notch radius, c is the notch half-length, and σ is the applied stress. Experience also indicates that below some critical radius ρ_o, the fracture stress is insensitive to further reduction in radius, so that

$$\sigma_{max} = \sigma(1 + 2\sqrt{c/\rho_o}) \tag{5}$$

for $\rho \leq \rho_o$. For typical high strength metals ρ_o is in the range of 10^{-4} - 10^{-2} inches [15,16], and is proportional to the plastic zone size of a natural crack [17].

A meaningful value of K_Q can be obtained only if the radius of the notch introduced into the specimen is less than ρ_o. In the derivation of the classical stress field about a sharp crack which leads to the definition of K_Q, it is assumed that the crack tip is infinitely sharp, and that any zone of inelastic behavior is very small compared to the crack length [18]. The stress field at the tip of a sharp crack in a typical anisotropic material is shown, in Reference [6], to deviate significantly from the classical $1/\sqrt{r}$ singularity at a distance ahead of the

crack equal to a small fraction of the total crack length. Thus, the existence of a zone of inelastic behavior at the crack tip, which is of the same order of magnitude in size as the crack length, would be expected to destroy the classical stress singularity and render the calculated value of K_Q meaningless. However, the nominal stress at fracture might still vary with $\sqrt{c}$ as in Equation (4) if most of the specimen remained elastic.

Figure 7 gives the variation in fracture stress with notch radius for a Style 61 woven roving/chopped mat reinforced laminate. Designating a roving ply as R and a mat ply as M, the ply configuration of the material is M/R/M/R/M which will be the case for all 5 ply roving/mat laminates discussed; in this case the roving is oriented with the 0°, or fill direction parallel to the load, and the warp direction at 90°, perpendicular to the load. In all of the following cases the angle given for the roving represents the angle between the load direction and the fill direction. The results in Figure 7, which are similar to those in Reference [6] for graphite/epoxy, indicate that the applied stress at fracture is relatively constant or even decreases slightly as the notch tip radius increases up to approximately 0.10 inches, and then increases as the radius becomes larger. The effective stress concentration of the sharpest notch is relatively low, as the average stress on the net cross-section between notches is approximately 60% of the ultimate tensile strength

for the one inch notch length.

The value of ρ_o implicit in Figure 7 is approximately 0.10 inch, one to three orders of magnitude greater than that reported for high strength metals, and consistent with the dimensions of the subcracking zone in Figure 6. Although it is desireable to have the inherent bluntness of a natural crack in any material be as great as possible, the applicability of LEFM must be questioned for such a case. Despite the brittle character of the fracture, which occurs catastrophically with the entire sample behaving elastically except for the small damage region near the crack tip, the existence of a classical stress singularity at the crack tip seems unlikely.

Figure 8 presents the effect of the notch shape on the fracture stress; as expected, the notch flank angle has little influence on the fracture stress over a broad range. The data in Figures 7 and 8 indicate that for a notch several tenths of an inch long, the fracture stress is almost completely insensitive to the shape of the notch, even to the extreme case of a circular hole, as was indicated in Reference [5] for a 181-style fabric reinforced laminate. The length of the notch is of great importance, however, as will be indicated in the next section. The relative insensitivity of the fracture stress to notch radius is convenient, since no difficulty is encountered in introducing a naturally sharp crack into the sample for testing. This is contrary to experience with homogeneous materials.

FRACTURE CRITERIA AND SPECIMEN SIZE EFFECTS

The preceding comments and data have raised doubts about the applicability of classical LEFM and the meaning of K_Q for fiber reinforced plastics. The difficulty in measuring the stresses immediately local to the crack tip precludes direct evidence to clarify the question; however, the practical utility of any fracture criterion can be determined by testing specimens of varying size and crack length to determine whether the fracture stress is accurately predicted by the criterion for all cases.

The data given in the previous section suggests another brittle fracture criterion which is not based on the classical stress singularity. Following the concept originally suggested by Neuber [17] and Kuhn [19] for metals, a generalized version of Equation (5) may be used for cracks with $\rho \leq \rho_o$ given by:

$$\sigma_{UTS} = \sigma_f(1 + q\sqrt{c}) \tag{6}$$

where σ_{UTS} is the ultimate tensile strength, and q is a generalized stress concentration parameter which includes the effects of inherent radius, ρ_o, specimen shape (analogous to Y in Equation (1)), and, for anisotropic materials, the effect of modulus. For high strength metals $q\sqrt{c} >> 1$, and Equation (6) reduces to a simple criterion where the fracture stress is inversely proportional to $\sqrt{c}$ as in the classical Equation (1). The two criteria are not identical

for many composite materials, however, since $q\sqrt{c}$ is of the same order of magnitude as unity.

Figures 9(a) - 9(h) give the results of notched tension tests on laminates constructed of Style 779 woven roving/chopped mat, woven roving alone, and chopped mat alone, with various orientations of the woven roving. Specimens of 2, 4 and 6 inch width were tested with 2c/w ratios of 0.25 and 0.50. In each case the solid line represents the classical LEFM criterion, while the dashed line represents the generalized stress concentration criterion, with the average of K_Q or q for all specimen sizes used to obtain the equation of the line.

From the results in Figures 9(a) - 9(h), it appears that either criterion fits the data reasonably well for large cracks, although the generalized stress concentration criterion appears to be in agreement with the data over a broader range of crack lengths, particularly for short cracks, as would be expected.

Figure 10 gives the variation of K_Q and q with woven roving orientation for the roving/mat laminates. Since the woven roving is not balanced in the warp and fill directions (it has more fibers in the warp), the data are not symmetric about 45°. The variation in toughness with roving orientation for this five ply, M/R/M/R/M material is not great, however, and the fracture surface appearance was similar in all cases. The only noticeable effect of roving orientation was on the direction of crack propagation:

the crack typically propagated at approximately half of the orientation angle. For example, the crack deviation from the original notch direction was approximately 22° for the 45° roving orientation. The deviation from colinear crack growth further violates the assumptions of Equation (1) for LEFM.

Figure 11 shows the two extreme cases observed for sensitivity to notches: woven roving oriented at 90° and at 45°. For all specimen sizes, the 45° case fails at a stress on the net cross-sectional area of almost precisely the ultimate strength, while even small cracks reduce the net section strength considerably for the 0° case. The behavior in the 45° case is unique among the materials tested in this study, and was apparently the result of severe inelastic deformation and cracking across the entire specimen prior to fracture. Similar behavior is reported for $\pm$45° graphite/epoxy laminates as well as for higher fiber orientations such as $\pm$75° in Reference [6].

The variation of K_Q with specimen width is plotted for several materials in Figure 12 using the data given in Figure 9. As described by Owen and Bishop [1] for similar laminates, the value of K_Q is found to increase with the width of the specimen. Following the procedure used with metals [18], which has also been employed by Owen and Bishop, it is possible to reduce or eliminate this variation with width by correcting the crack length used in the calculation of K_Q, as indicated in Figure 13. The

crack length correction, Δc, is added to the actual crack length in Equation (1) to obtain the corrected K_Q. Although the value of Δc used with metals is based on the effect of the plastic zone size on the elastic stress field, the procedure takes on the characteristics of simple curve fitting in the case of composites, and the correction factors may become unrealistically large.

The generalized stress concentration criterion, while providing good agreement with the data, is difficult to interpret. Figure 10 indicates a value for q in the range of 1.6 - 2.1 for the roving/mat laminates; neglecting the effects of anisotropy, this results in an unrealistically high value of ρ_o when q is compared to Equation (5). While the reasons for this discrepancy are not clear at this time, it is thought that the generalized stress concentration concept may be more consistent with the fracture characteristics of composite materials than is the K_Q concept, and should be further explored.

LAMINATE THICKNESS EFFECTS

The fracture toughness of metals is known to be a strong function of thickness [20]; thin specimens under plane stress conditions yield more readily at the crack tip and display higher toughness, while for thick specimens yielding is constrained under plane strain conditions, resulting in lower thoughness. In earlier descriptions of the origines of toughness for fiber reinforced plastics [4,5], crack propagation even for very thin specimens was characterized as blunting of the main crack by subcracking, and brittle tensile failure of

the ligaments at the crack tip so that no thickness effects due to variations in the triaxial stress field contraint on plastic flow are anticipated.

Figures 14 and 15 indicate that the value of K_Q obtained for 181-style fabric and roving/mat reinforced composites is almost completely insensitive to thickness over a broad range (see Reference [21] for more details on the 181-style fabric tests). The roving/mat laminates were of the ply configuration M/R/M/R/M/..../R/M, and the orientation for both materials was 0°.

The results in Figures 14 and 15 suggest that the complications which thickness effects incur on fracture toughness testing of metals are not to be expected for this class of composites. Figure 16 indicates, however, that thickness complications can exist for some composites, particularly those with unidirectional plies. In this case the origins of the effect are clearly indicated in Figure 17. When the plies on the outside surfaces are oriented with fibers in the load (0°) direction, the split length is excessive, measuring several inches compared to the usual tenth of an inch when each 0° ply is constrained by a 90° ply on either side (the outside plies are oriented at 90°). In the case with each 0° ply constrained by a 90° ply on either side, the value of K_Q decreases only slightly with thickness, perhaps because of problems in curing the thicker sections. The interior 0° plies of the specimens with 0° surface plies are also under con-

straint from a 90° ply on either side, so only the surface plies display different behavior. If a value of K_Q for the surface 0° plies is obtained from the 3 ply (0°/90°/0°) case, and a value of K_Q is obtained for constrained 0° plies from the cases with 90° surface plies, then a simple rule of mixtures formula gives the expected value of K_Q normalized to consider the effect of 0° plies only, K_Q^o, as:

$$K_Q^o = \frac{2(K_Q^o)_{surface} + (n-2)(K_Q^o)_{interior}}{n} \qquad (7)$$

where

$$K_Q^o = K_Q\left(\frac{\text{total number of plies}}{\text{number of 0° plies}}\right)$$

and n is the number of 0° plies.

Figure 16 indicates fair agreement between Equation (7) and the measured results, with most of the deviation for thicker specimens probably due to the curing problems which lower the toughness of both types of laminates. The effect of thickness on other ply configurations, particularly those which fail in a shear buckling mode, are not known, but may also be significant.

STRAIN RATE AND TEMPERATURE EFFECTS

The effects of strain rate and temperature have been investigated for Scotchply and roving/mat laminates, and the results are found to be contrary to experience with metals. Figure 18 shows that K_Q for (0°/90°) Scotchply

and K_Q and G_Q for roving/mat increase steadily with deflection rate. Figure 19 shows a similar increase with decreasing temperature for the same materials, as well as for (45°/-45°/0°/-45°/45°) Scotchply, which fails in the shear buckling mode. Variations with rate and temperature appear to be similar to the published variations for strength and modulus of 0°/90° Scotchply [22], and, more meaningfully, the data indicate similar rate effects to those measured for E-glass fibers alone [23]. The apparent close dependence of the laminate toughness on the fiber modulus and strength is consistent with the toughening mechanism described earlier, and suggests a more efficient use of composites in low temperature, high rate applications than under the reverse conditions which tend to favor the application of metals.

EFFECTS OF MATERIAL COMPOSITION

The data presented in earlier sections of this paper indicate that the style and orientation of reinforcement may have a significant effect on the toughness, and Reference [6] indicates that an order of magnitude variation in K_Q with fiber orientation is possible. Figure 16 also indicates that the arrangement of plies may have a significant effect, particularly in the case of unidirectional plies, and earlier work has indicated that an order of magnitude increase in G_Q is possible by varying the ply

stacking configuration [5]. K_Q and G_Q have also been shown [4,5] to increase in proportion to the fiber volume fraction as do the strength and modulus.

Table 2 indicates that the properties of the matrix material have very little effect on the toughness of the composite. The various matrices represent a difference of approximately a factor of 40 in fracture surface work between polyester and CTBN modified epoxy [24], with only a minor effect on composite toughness detectable. This again indicates that the fiber properties determine the toughness of the composite. Apparently the growth of subcracks which blunt the main crack is controlled more by the constraint of adjacent plies than by the toughness and adhesion properties of the matrix.

CONCLUSIONS

The toughness of FRP laminates derives from the growth of subcracks which blunt the main crack and reduce the concentration of stress. The validity of classical linear leastic fracture mechanics is doubtful due to the inherent bluntness of the crack, and a generalized stress concentration criterion may provide a conceptually sound and practical alternative. The fracture toughness of FRP laminates tends to increase with decreasing temperature and increasing strain rate, and is insensitive to thickness in many cases; each of these characteristics is contrary to experience with metals.

Fracture toughness is also sensitive to fiber orientation and ply stacking arrangement, increases in proportion to fiber volume fraction and is insensitive to matrix toughness.

ACKNOWLEDGEMENTS

The general research program on the fracture behavior of fibrous reinforced composites, from which this report dervies, receives support from The Dow Chemical Company, the Air Force Materials Laboratory (USAF Contract F33615-72-C-1686), the Office of Sea Grant (NOAA, NG43-72) and the M.I.T. Center for Materials Science and Engineering (NSF Contract GH-33653). This support is gratefully acknowledged by the authors.

Several of the results presented in this paper were obtained by students in courses 1.10, 1.471, and 1.472 at M.I.T., and their assistance is gratefully acknowledged.

REFERENCES

1. M.J. Owen and P.T. Bishop, "Critical Stress Intensity Factor Applied to Glass Reinforced Polyester Resin," J. Composite Materials, Vol. 7, (April 1973), p. 146.

2. E.M. Wu and R.C. Reuter, Jr., "Crack Extension in Fiberglass Reinforced Plastics," Univ. of Illinois, TAM Report 275 (1965).

3. D.B. Hiatt, "Fracture of Prenotched Unidirectional Glass Fiber Reinforced Composites," S.M. Thesis, MIT Dept. of Mech. Engr. (1970).

4. F.J. McGarry and J.F. Mandell, "Fracture Toughness of Fibrous Glass Reinforced Plastic Composites," Proc. 27th Reinforced Plastics/Composites Div., SPI (1972), Section 9A.

5. F.J. McGarry and J.F. Mandell, "Fracture Toughness Studies of Fiber Reinforced Plastic Laminates," Proc. Special Discussion of Solid-Solid Interfaces, Faraday Division of The Chemical Society, Nottingham, England (1972).

6. J.F. Mandell, S.S. Wang, and F.J. McGarry, "Fracture of Graphite Fiber Reinforced Composites," Air Force Materials Laboratory Report AFML-TR-73-142 (July 1973).

7. J. Cook and J.E. Gordon, "A Mechanism for the Control of Crack Preparation in All Brittle Systems," Proc. Roy. Soc. A282 (1964), p. 508.

8. W.F. Brown, Jr. and J.E. Srawley, "Commentary on Present Practic," Review of Developments in Plane Strain Fracture Toughness Testing, ASTM STP 463, American Society for Testing and Materials, 1970, p. 216.

9. D.L. Bowie, "Rectangular Tensile Sheet with Symmetric Edge Cracks," Paper 64-APM-3, ASME (1964).

10. B. Gross and J.E. Srawley, "Stress Intensity Factors by Boundary Collocation for Single-Edge Notch Specimens Subject to Splitting Forces," NASA Technical Note D-3295 (1966).

11. M.F. Kanninen, "An Augmented Double Cantilever Beam Model For Studying Crack Propagation and Arrest," Int. J. of Fracture, Vol. 9, (1973), p. 83.

12. G.R. Irwen, "Analytical Aspects of Crack Stress Field Problems," TAM Report 213, Univ. of Illinois (1962).

13. A. Kelly, Strong Solids, Clarendon, Oxford (1966).

14. C.E. Ingliss, Trans. Naval Arch., Vol. 55, No. 1, p. 219.

15. J.H. Malherin, D.F. Armiento, and H. Marcess, "Fracture Characteristics of High Strength Aluminum Alloys Using Specimens with Variable Notch-Root Radii," Paper presented to Am. Soc. Mech. Engr. meeting, Philadelphia (1963).

16. "Fracture Testing of High-Strength Sheet Materials," Materials Research Standards, Vol. 1, (1966), p. 716.

17. H. Neuber, "Kerbspannungslehre," Berlin, Julius Springer (1937).

18. G.R. Irwin, "Analysis of Stresses and Strains Near the Tip of a Crack Traversing a Plate," Trans. ASME, J. App. Mech. (1957), p.361.

19. P. Kahn, "Colloquim on Fatigue; Stockholm, May 1955," (Ed. W. Weibull and F.K.G. Odquist) Berlin (Springer-Verlag) (1956), p. 131.

20. G.R Irwin, "Fracture Mode Transition for a Crack Traversing a Plate," Transactions, Am. Soc. Mech. Engr., Vol. 32, Series D (1960), p. 417.

21. W.J. Schulz, et al, "Fracture Toughness of FRP Laminated Plates," MIT Civil Engr. Report R70-1- (1970).

22. 3M Co., Technical Data Sheet for Type 1002 Scotchply (1963).

23. N.M. Cameron, "An Investigation into the Effects of Environmental Treatments on the Strength of E-Glass Fibers," TAM Report 274, Univ. of Illinois (1965).

24. G.B. McKenna, J.F. Mandell, and F.J. McGarry, "Interlaminar Strength and Toughness of Fiberglass Laminates," Proc. 29th Reinforced Plastics Technical and Management Conf., SPI, (February 1974), Paper 13-D.

TABLE I

FIBER VOLUME FRACTION AND PLY THICKNESS

Reinforcement or Material	Nominal Thickness per ply (in.)	Nominal Fiber Volume Fraction
Scotchply	0.010	0.50
Woven Roving	0.020	0.40
Chopped Mat	0.036	0.20
5 ply Roving/Mat	0.024	0.32
Variable Thickness Roving/Mat (Fig.15)	0.030	0.24
181-Style Fabric	0.0085	0.50

TABLE II

FRACTURE TOUGHNESS FOR SEVERAL MATRICES
REINFORCED WITH 9 PLIES OF 181 STYLE FABRIC
(DEN Specimens, 50% Fiber Volume Fraction)

Matrix	Fiber Orientation (Degrees)	Average K_Q (Ksi$\sqrt{in}$)
Polyester (Laminac 4173) (American Cyanamid Co.)	0°	18.3
	45°	16.0
Vinylester (Derakane 411-45) (Dow Chemical Co.)	0°	16.6
	45°	12.1
Epoxy (Epon 828/CAD) (Shell Chemical Co.)	0°	16.5
	45°	12.8
Epoxy + 10% CTBN Elastomer (B.F. Goodrich Co.)	0°	17.8
	45°	14.2

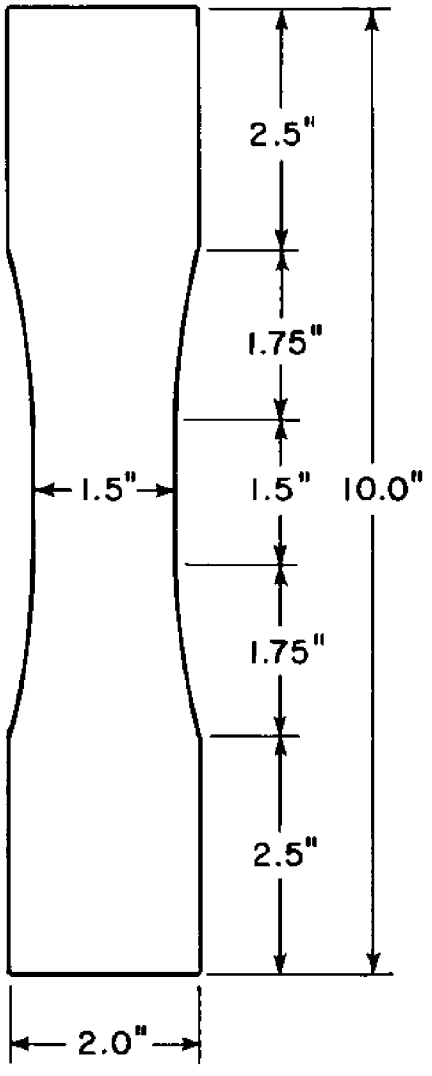

UNNOTCHED TENSION

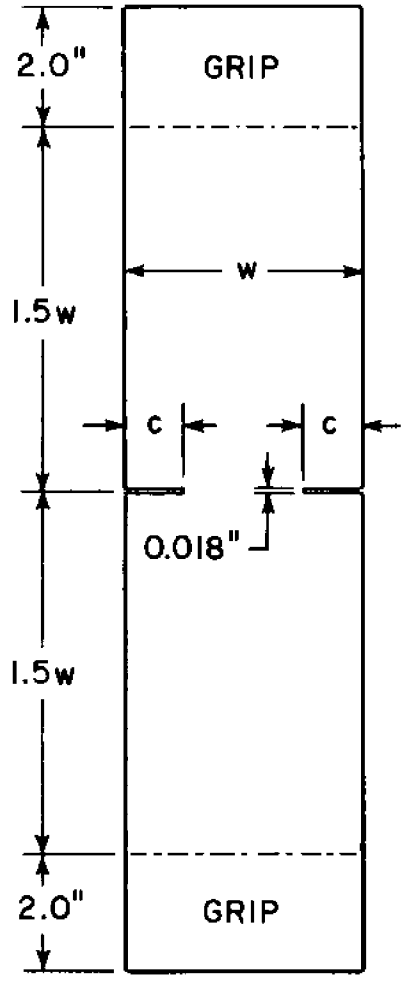

DOUBLE-EDGE-NOTCHED
TENSION
(DEN)

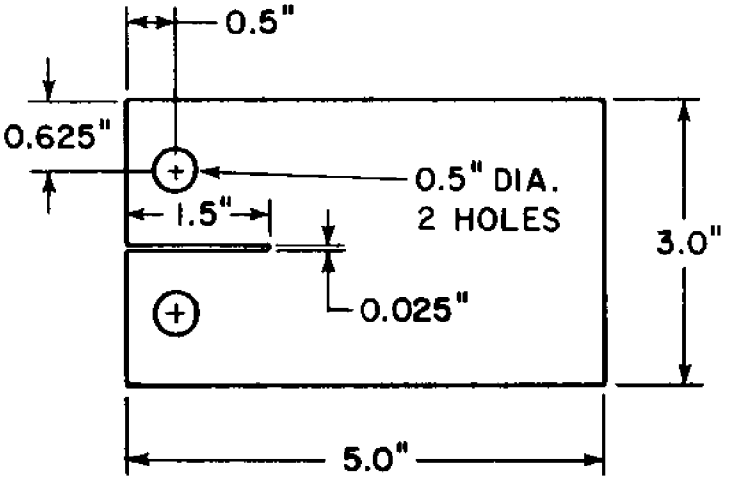

CLEAVAGE

FIGURE 1.

TEST SPECIMENS.

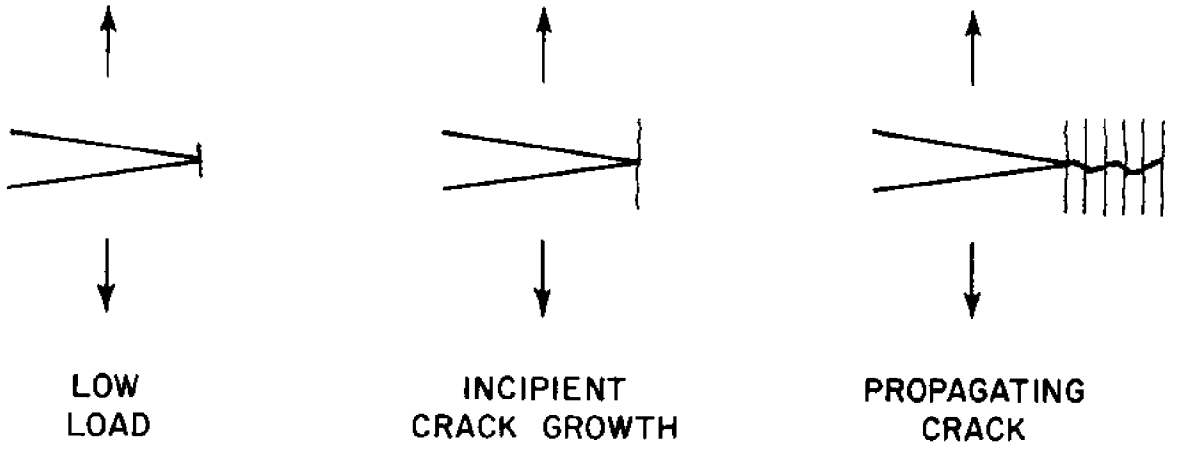

(a)
Schematic

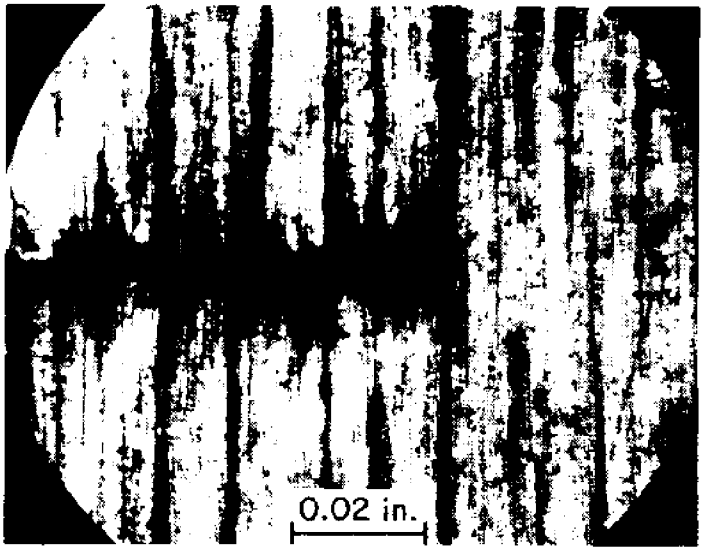

(b)
Crack Tip in 0°/90° Scotchply Laminate
(Transmitted Light)

FIGURE 2.

CRACK EXTENSION NORMAL TO FIBERS OF 0°/90° LAMINATE.

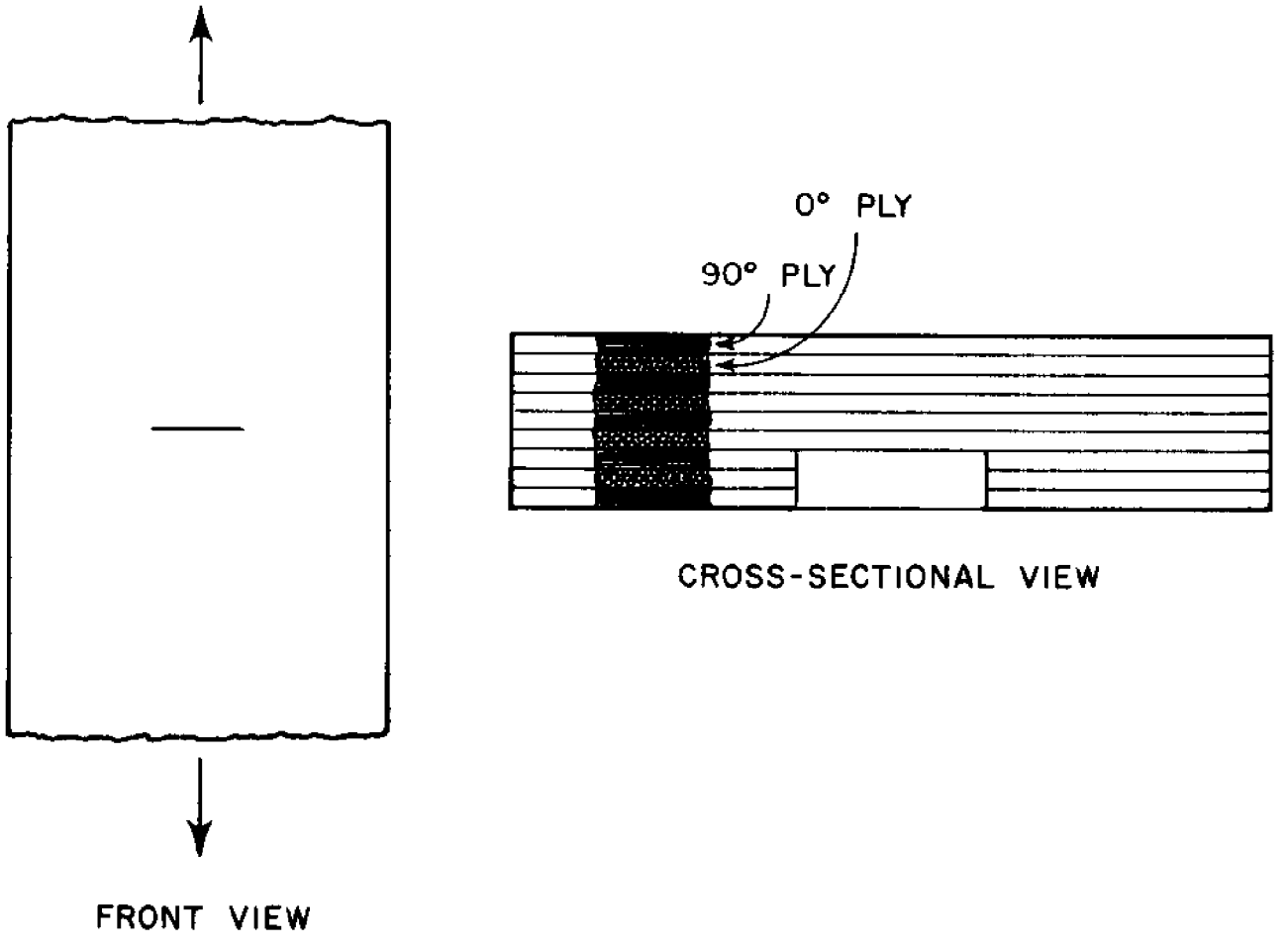

FIGURE 3.

SCHEMATIC OF 9 PLY, 0°/90° SPECIMEN WITH SURFACE CRACK, BEFORE LOADING.

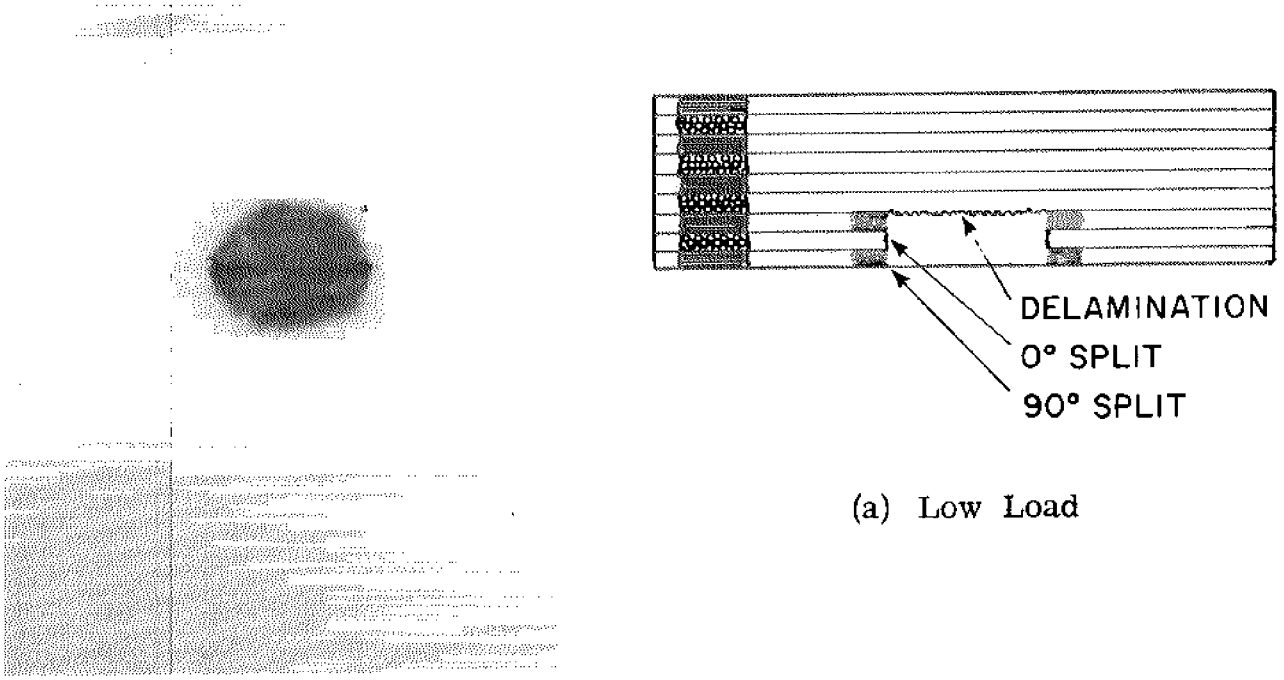

(a) Low Load

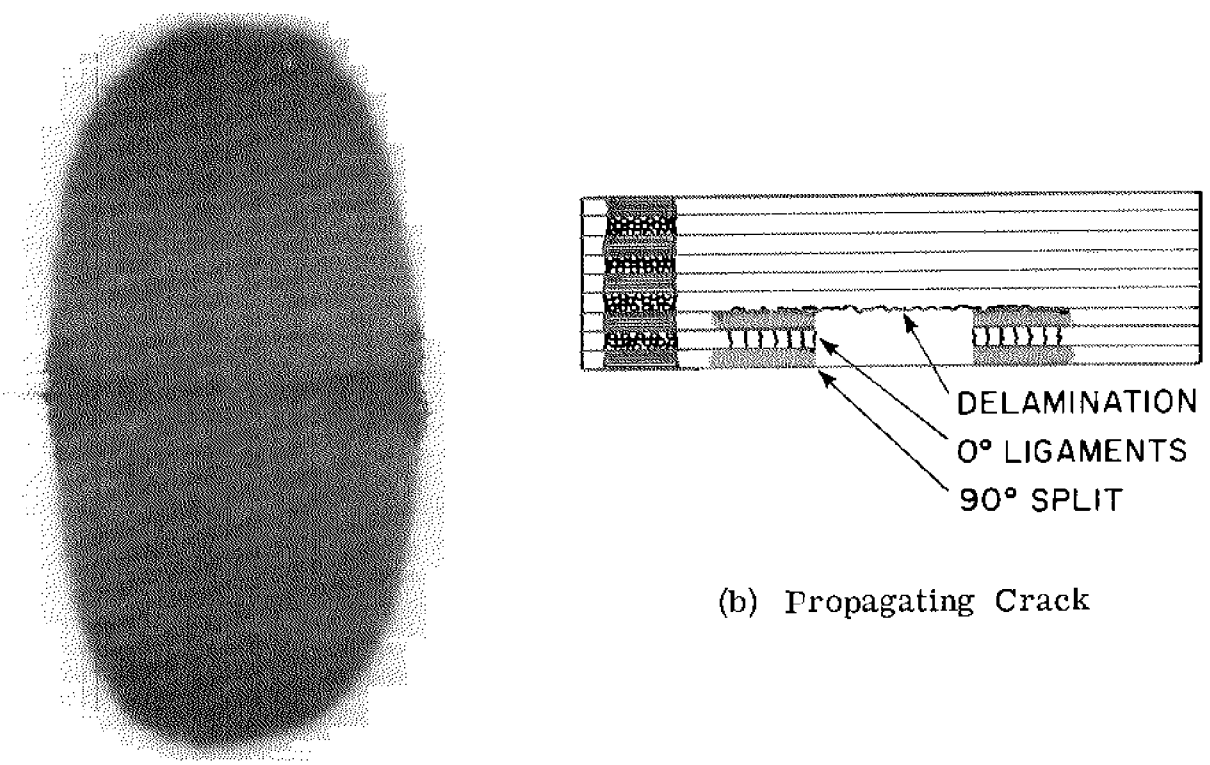

(b) Propagating Crack

FIGURE 4.

CROSS-SECTIONAL SCHEMATICS AND FRONT VIEW PHOTOGRAPHS OF INK-STAINED, SURFACE-CRACKED 0°/90° SCOTCHPLY SPECIMENS AFTER LOADING.

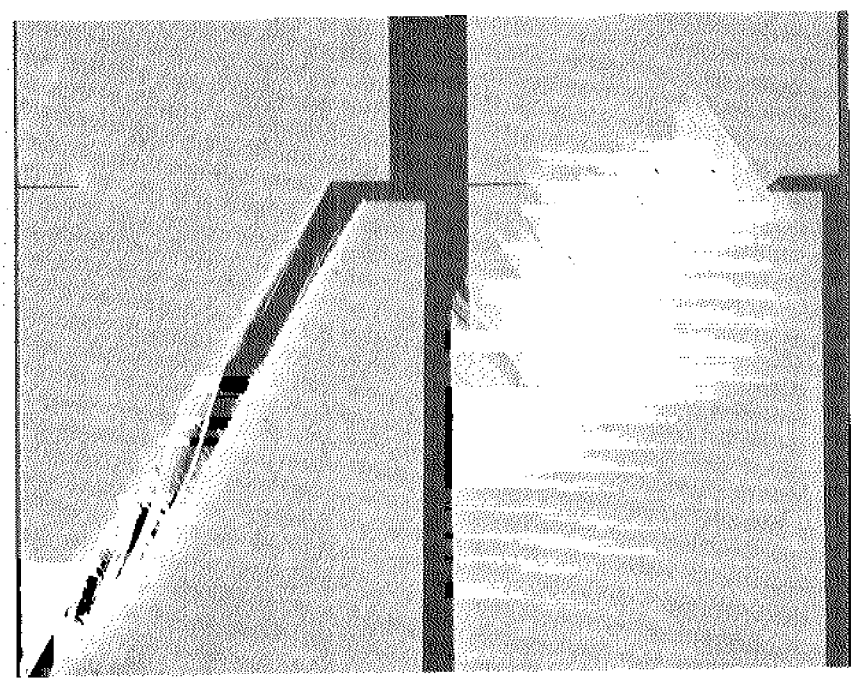

FIGURE 5.

FRACTURED SCOTCHPLY SPECIMENS INDICATING OPENING MODE FOR (30/-30/30/-30/30) LAMINATE (LEFT) AND SHEAR BUCKLING MODE FOR (-45/45/0/45/-45) LAMINATE (RIGHT).

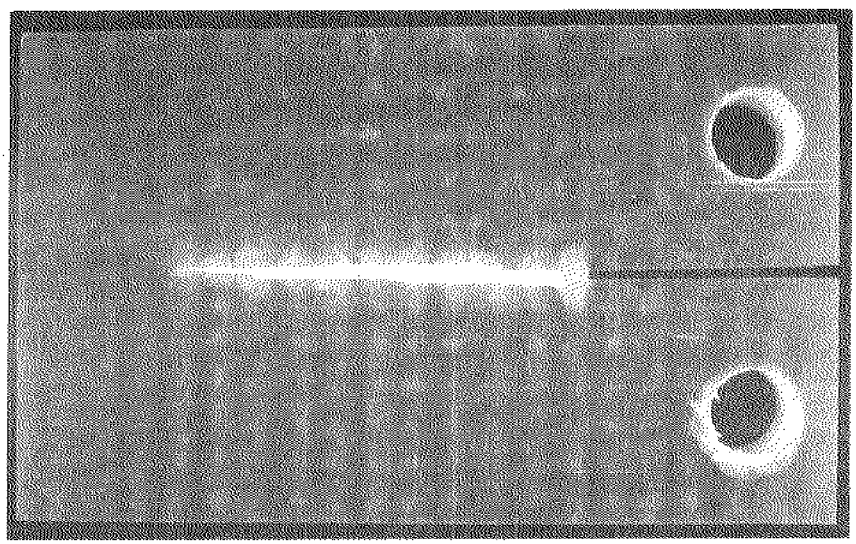

FIGURE 6.

CRACK PROPAGATING IN 0°/90° WOVEN ROVING/CHOPPED FIBER MAT REINFORCED POLYESTER LAMINATE.

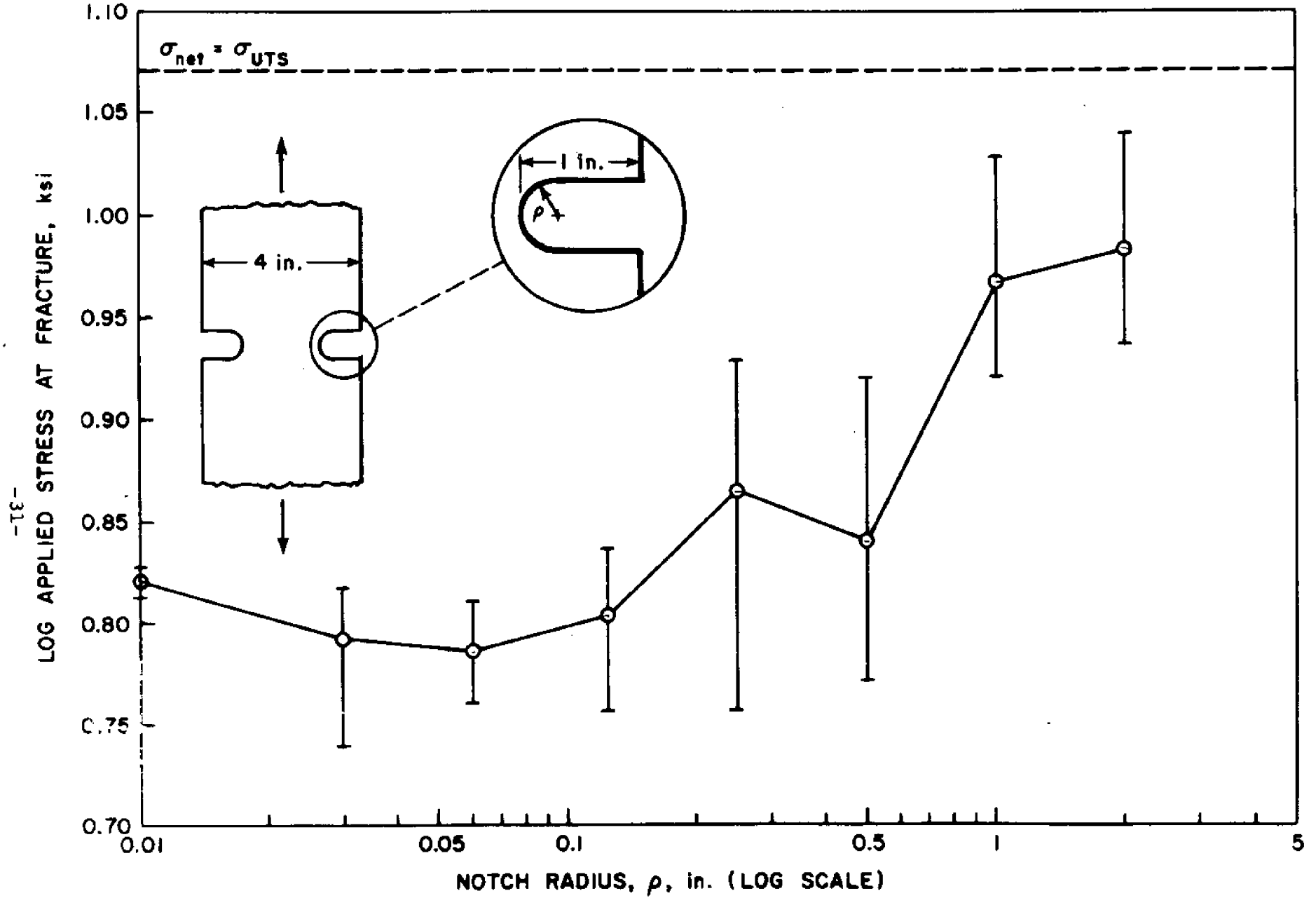

FIGURE 7.

EFFECT OF NOTCH RADIUS ON FRACTURE STRESS
FOR 5 PLY. 0° ROVING/MAT/POLYESTER.

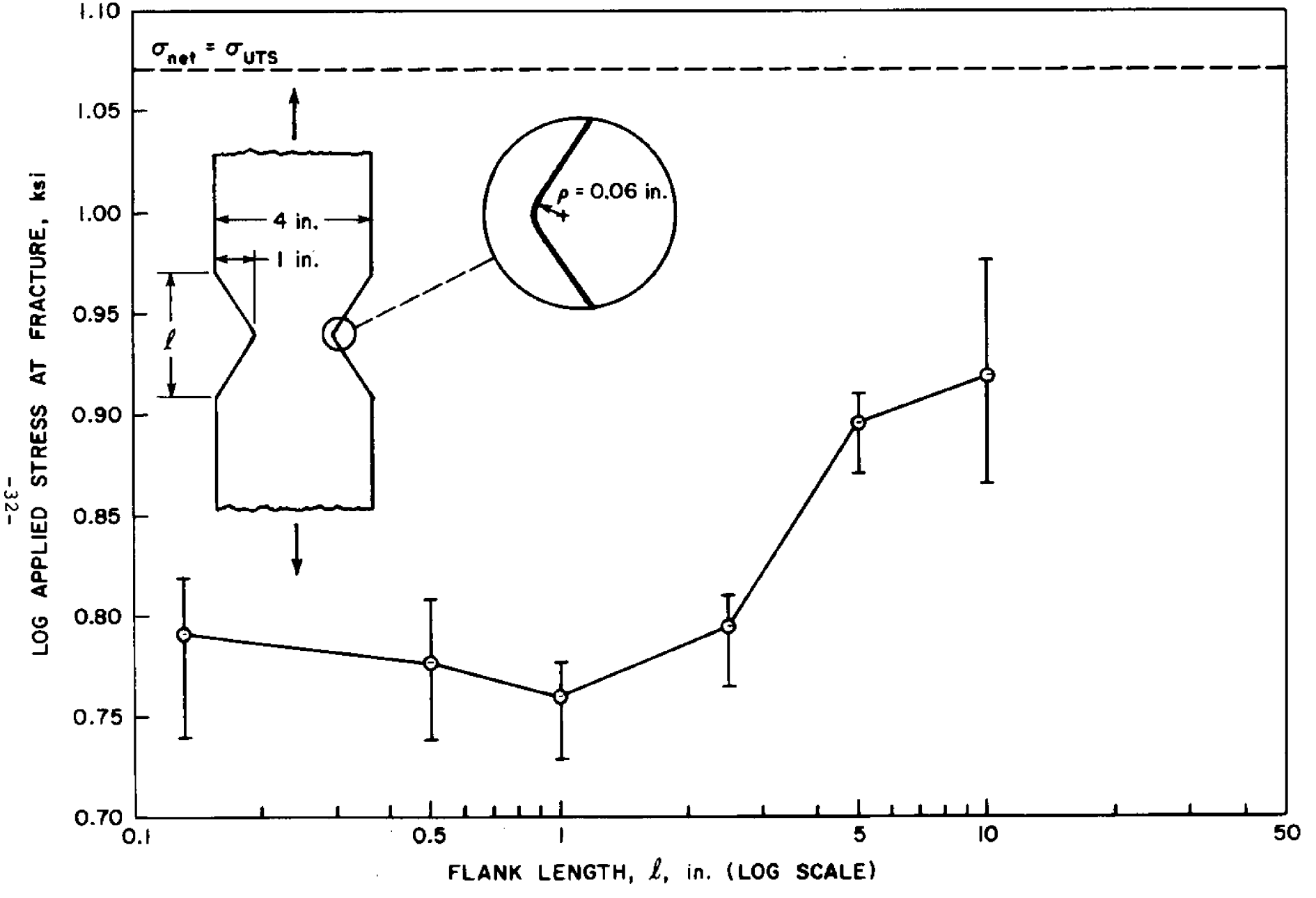

FIGURE 8.

EFFECT OF NOTCH FLANK LENGTH ON FRACTURE STRESS FOR 5 PLY, 0° ROVING/MAT/POLYESTER.

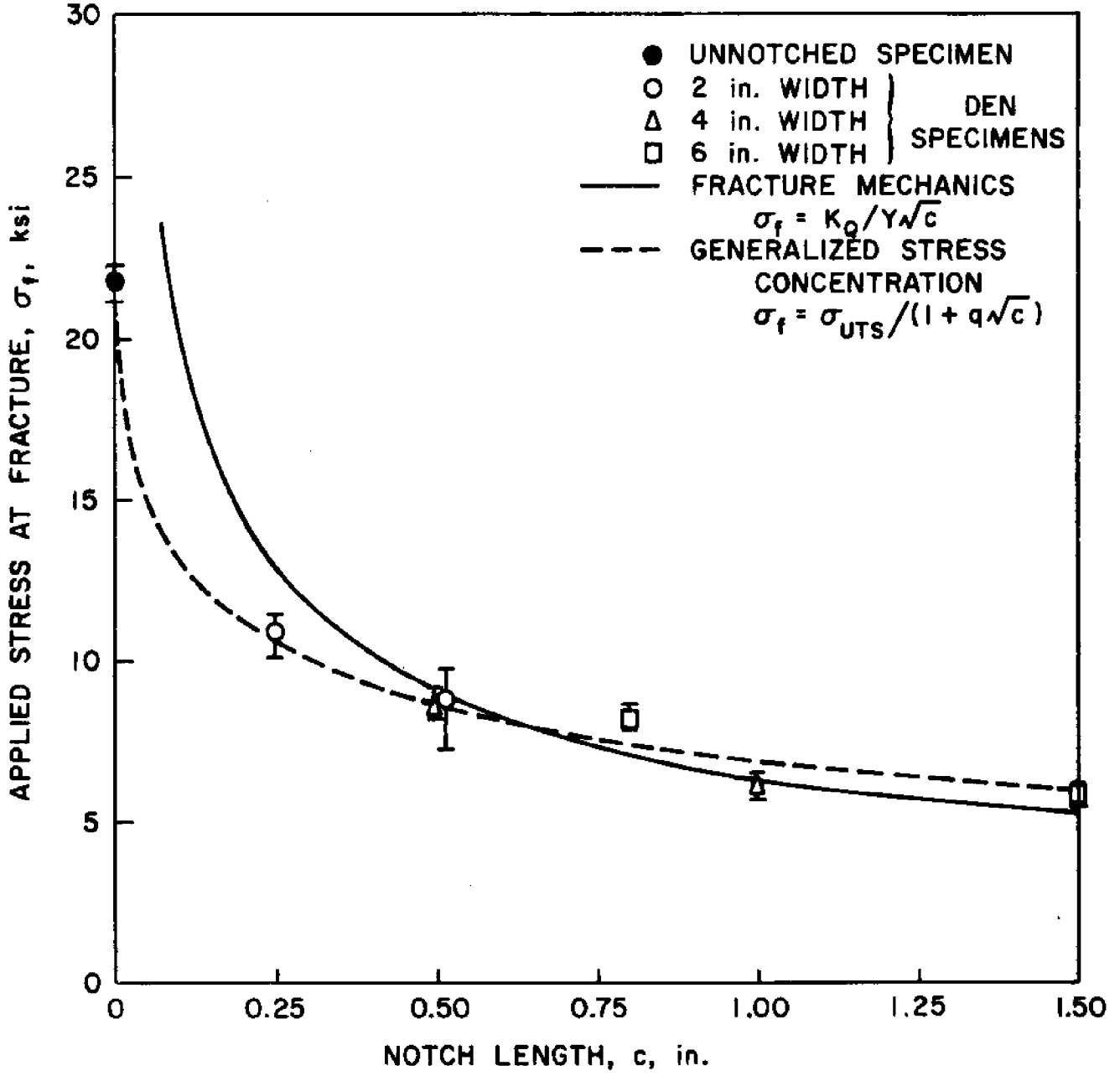

(a) 5 Ply, 0° Roving/Mat/Polyester

FIGURE 9.

VARIATION OF APPLIED STRESS AT FRACTURE WITH NOTCH LENGTH INDICATING ACCURACY OF FIT FOR FRACTURE TOUGHNESS AND STRESS CONCENTRATION CRITERIA, VARIOUS MATERIALS, DEN TEST.

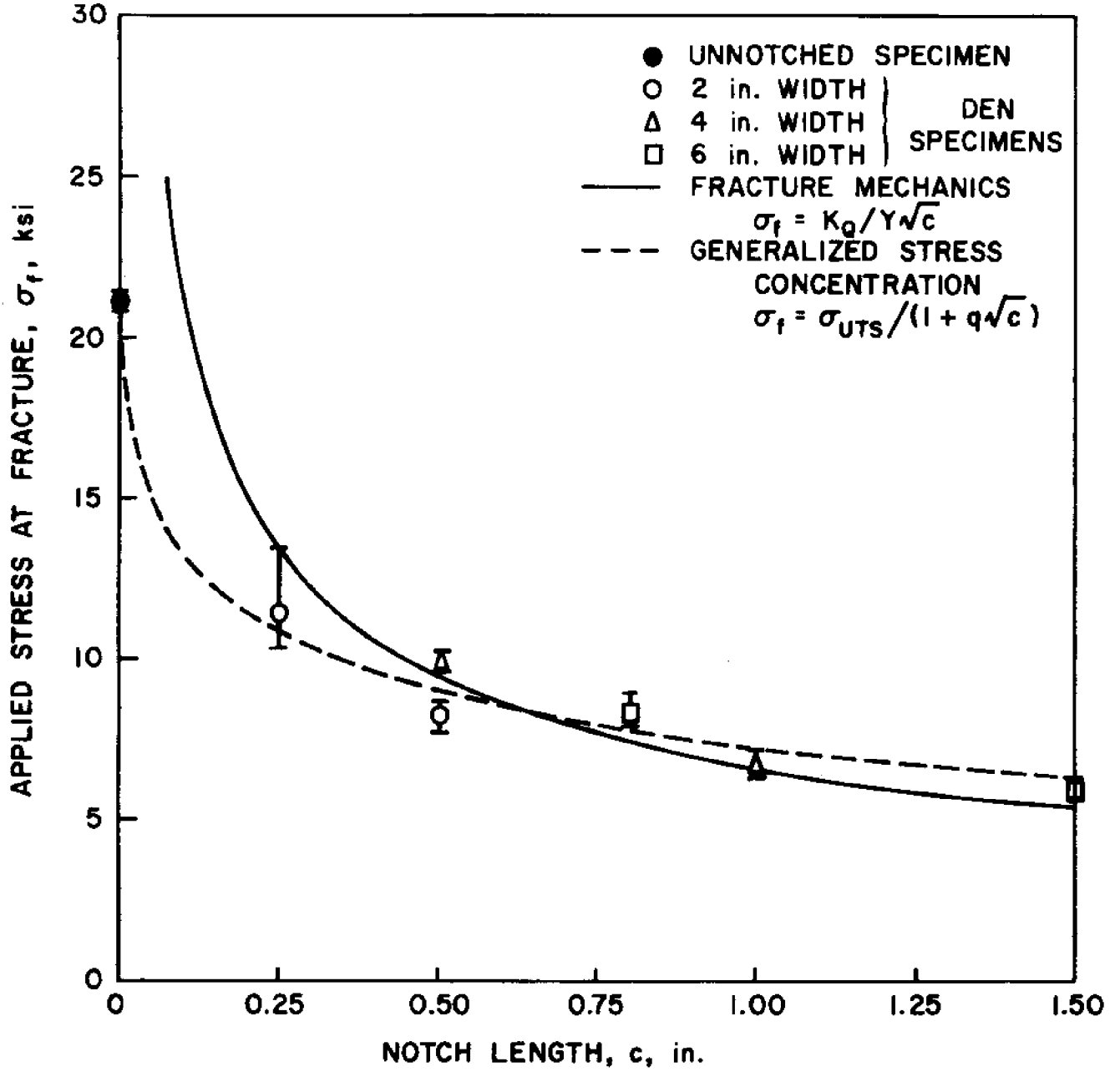

(b) 5 Ply, 30° Roving/Mat/Polyester

FIGURE 9 (continued).

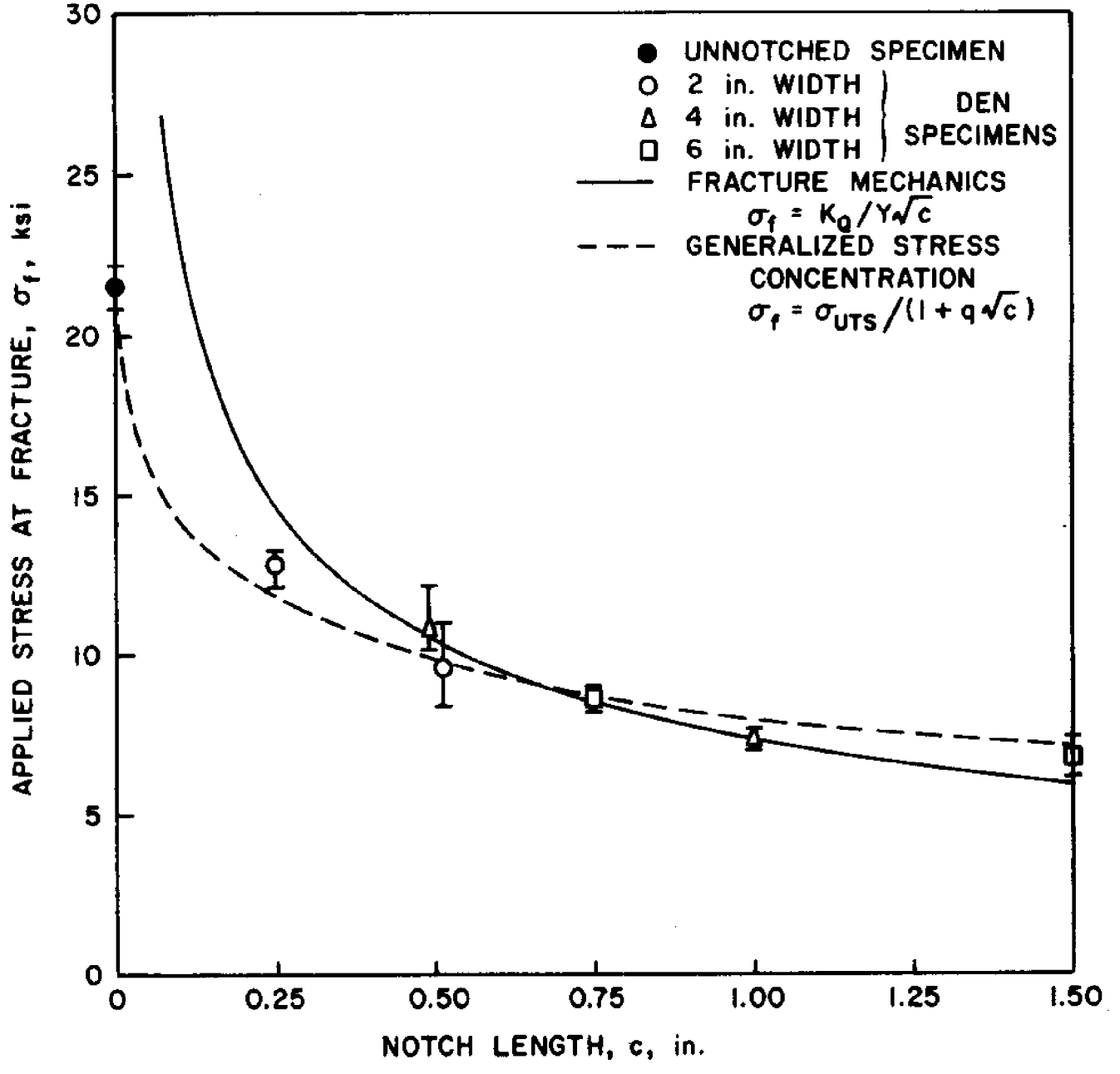

(c) 5 Ply, 45° Roving/Mat/Polyester

FIGURE 9 (continued).

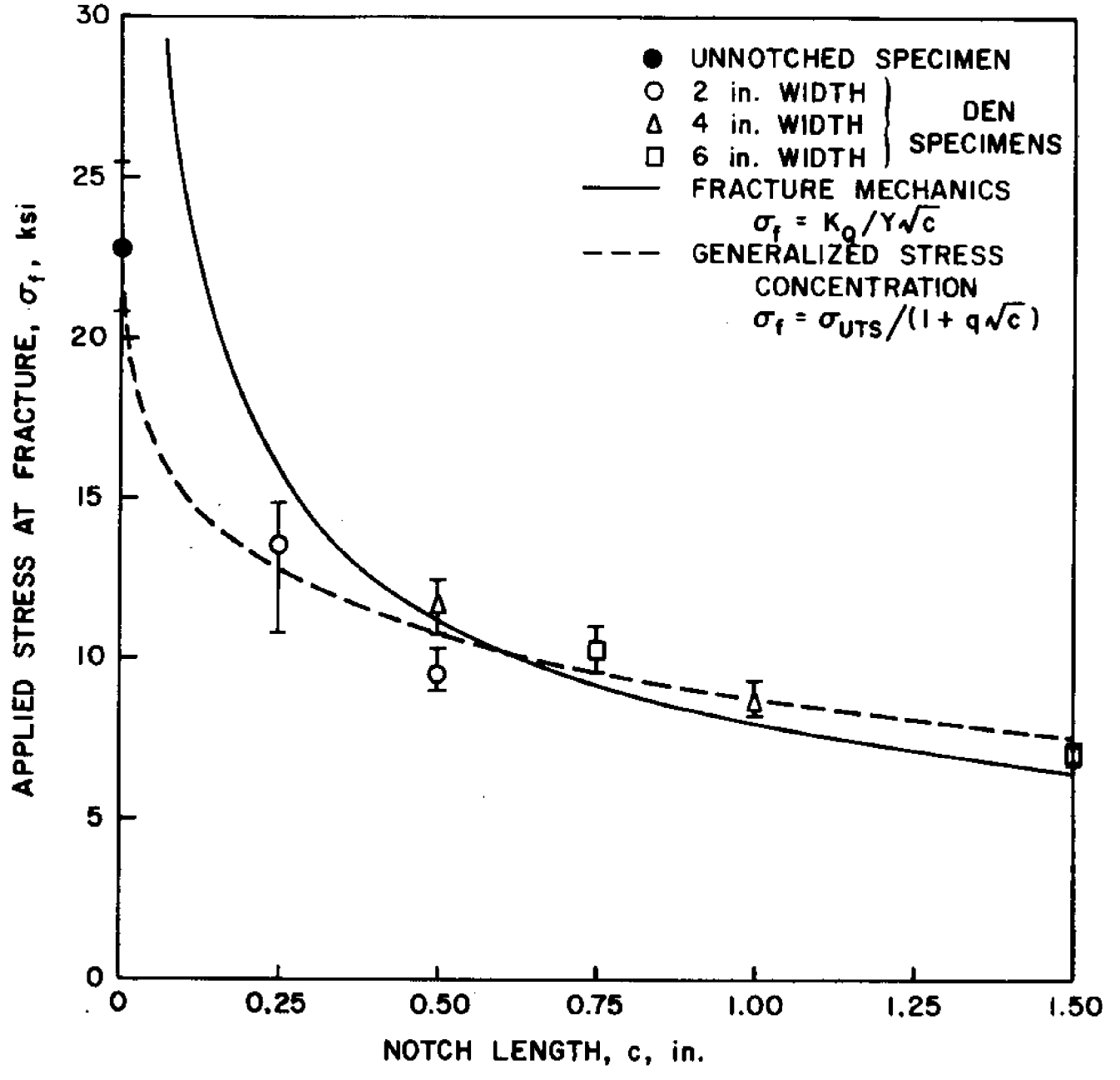

(d) 5 Ply, 60° Roving/Mat/Polyester

FIGURE 9 (continued).

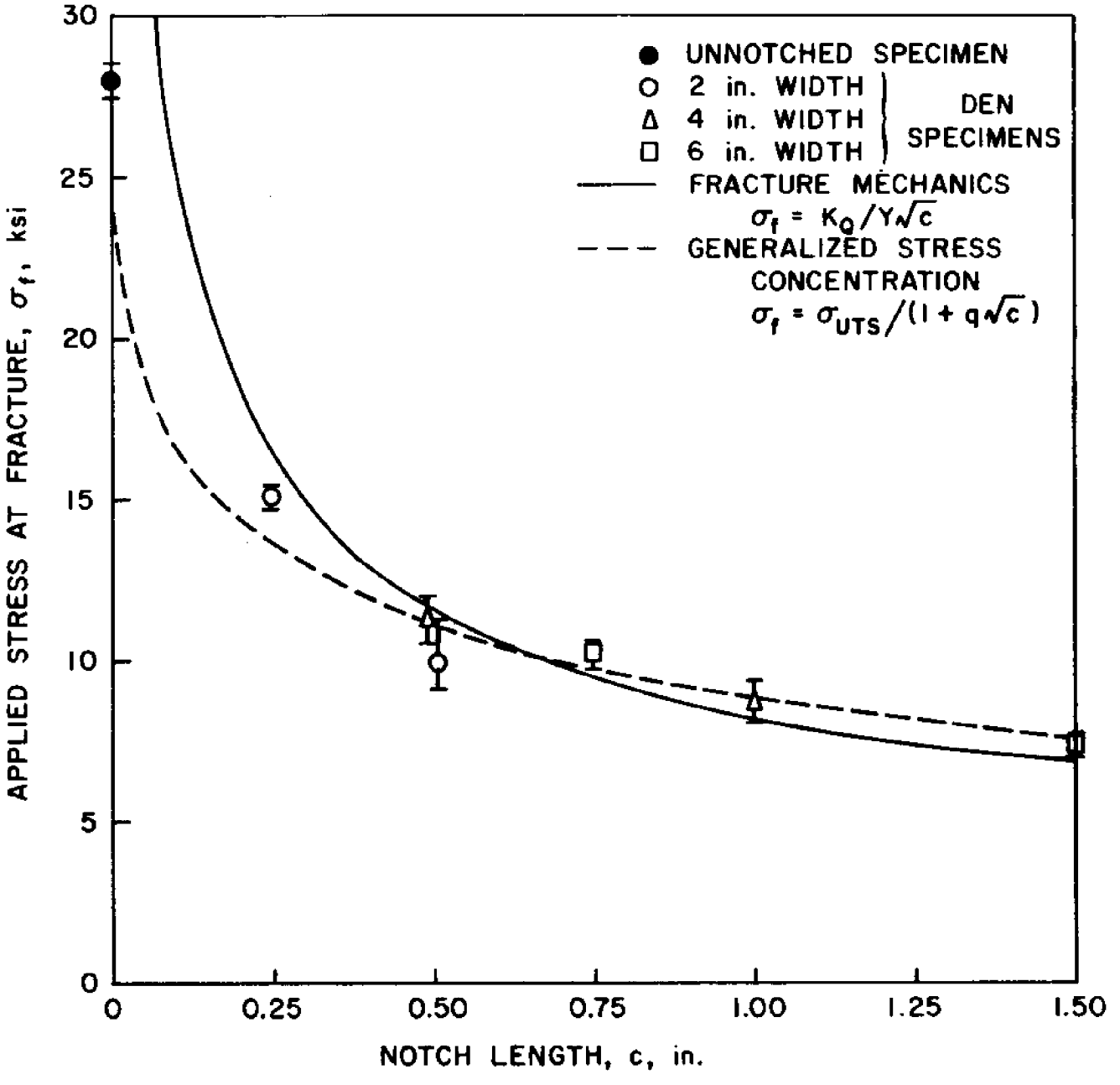

(e) 5 Ply, 90° Roving/Mat/Polyester

FIGURE 9 (continued).

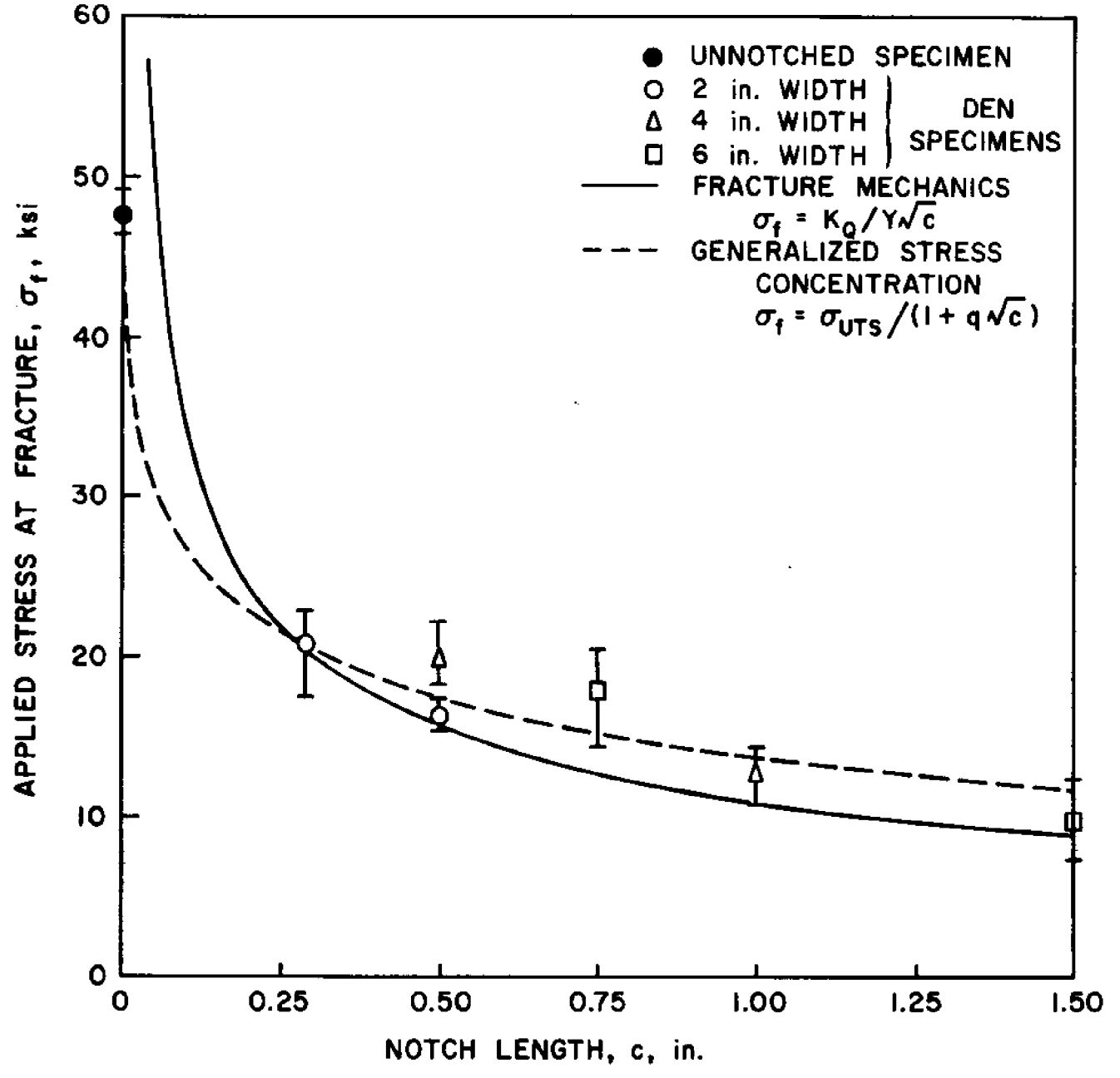

(f) 3 Ply, 90° Woven Roving/Polyester

FIGURE 9 (continued).

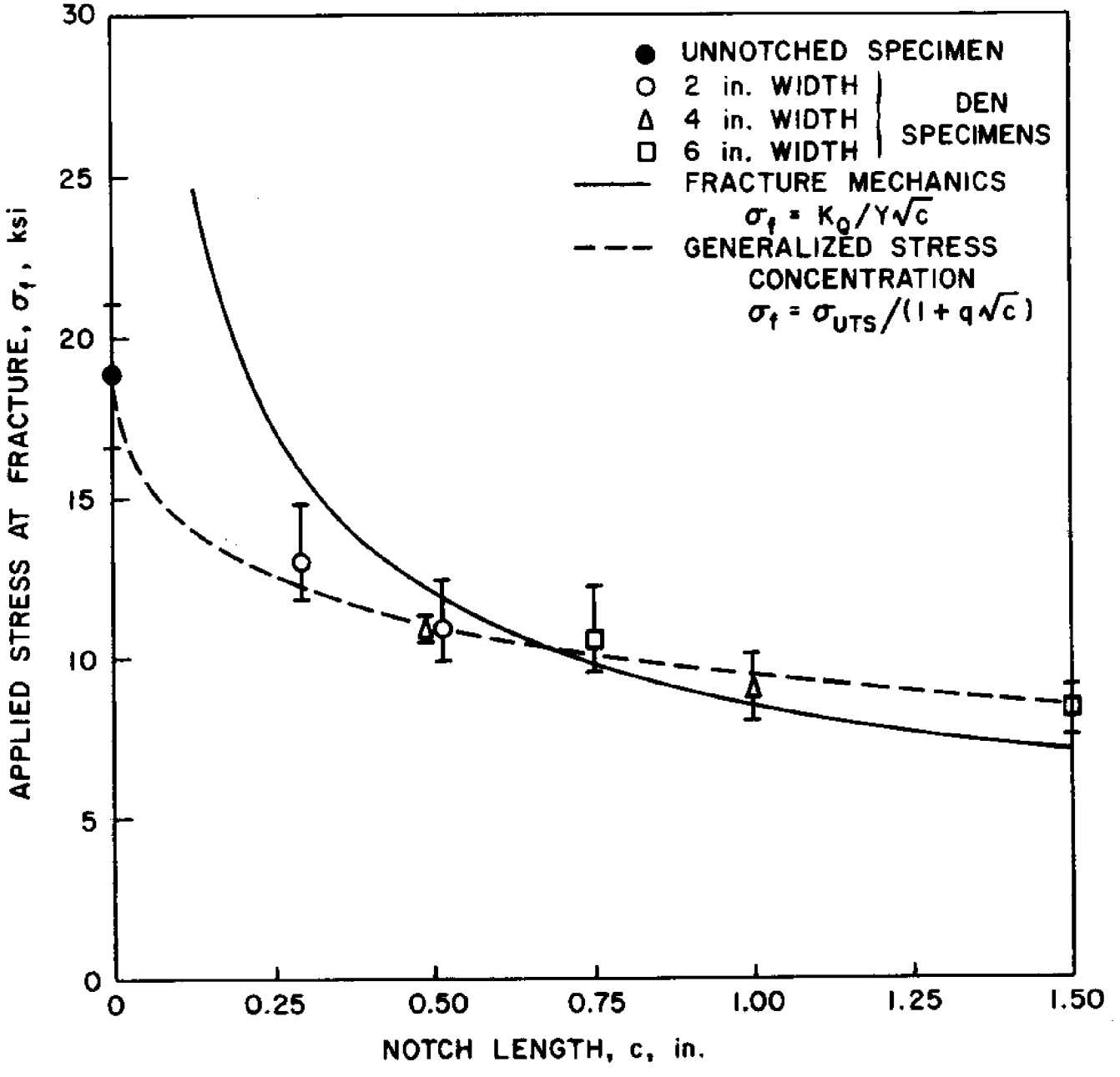

(g) 3 Ply, 45° Woven Roving/Polyester

FIGURE 9 (continued).

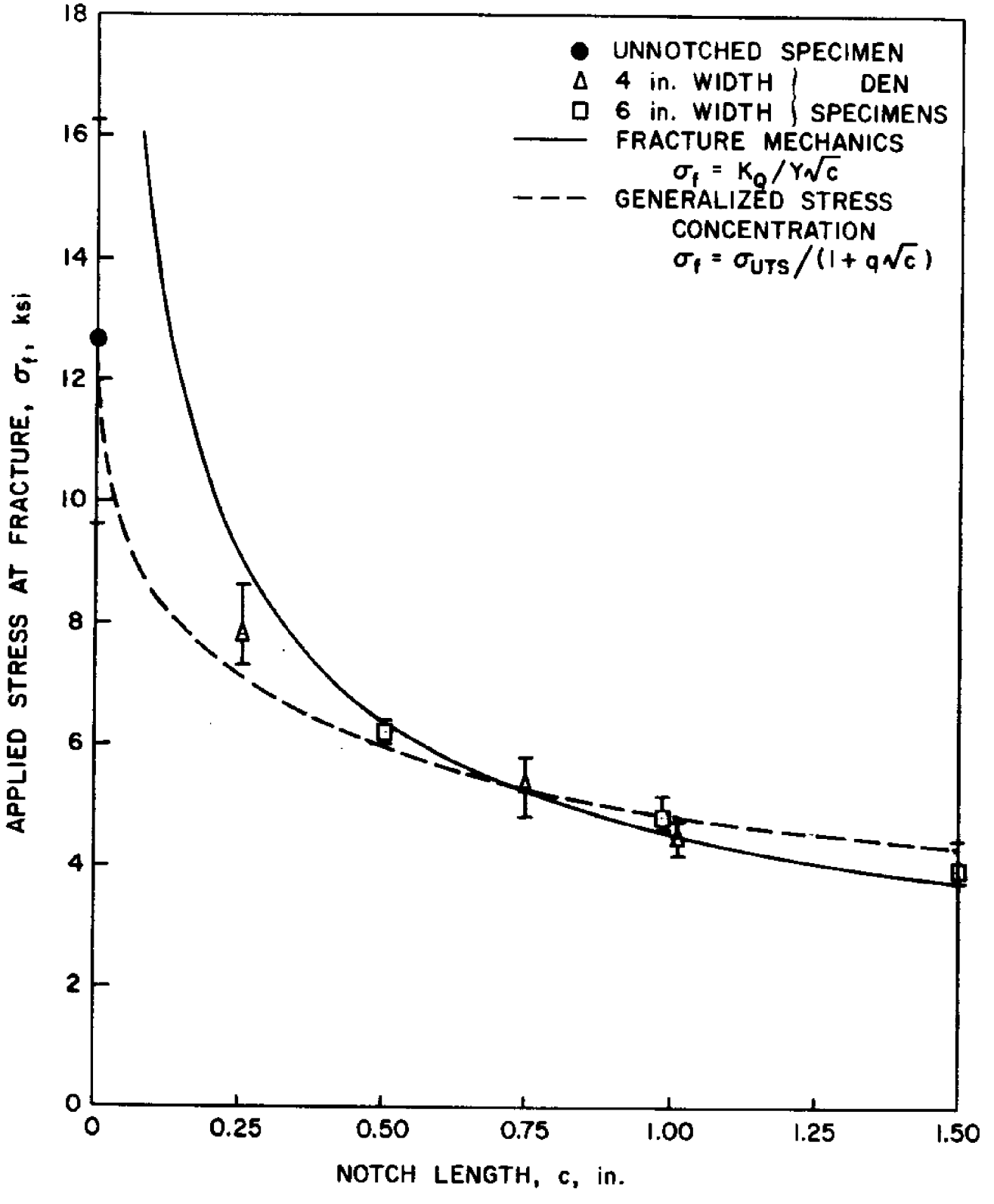

(h) 5 Ply Chopped Mat/Polyester

FIGURE 9 (continued).

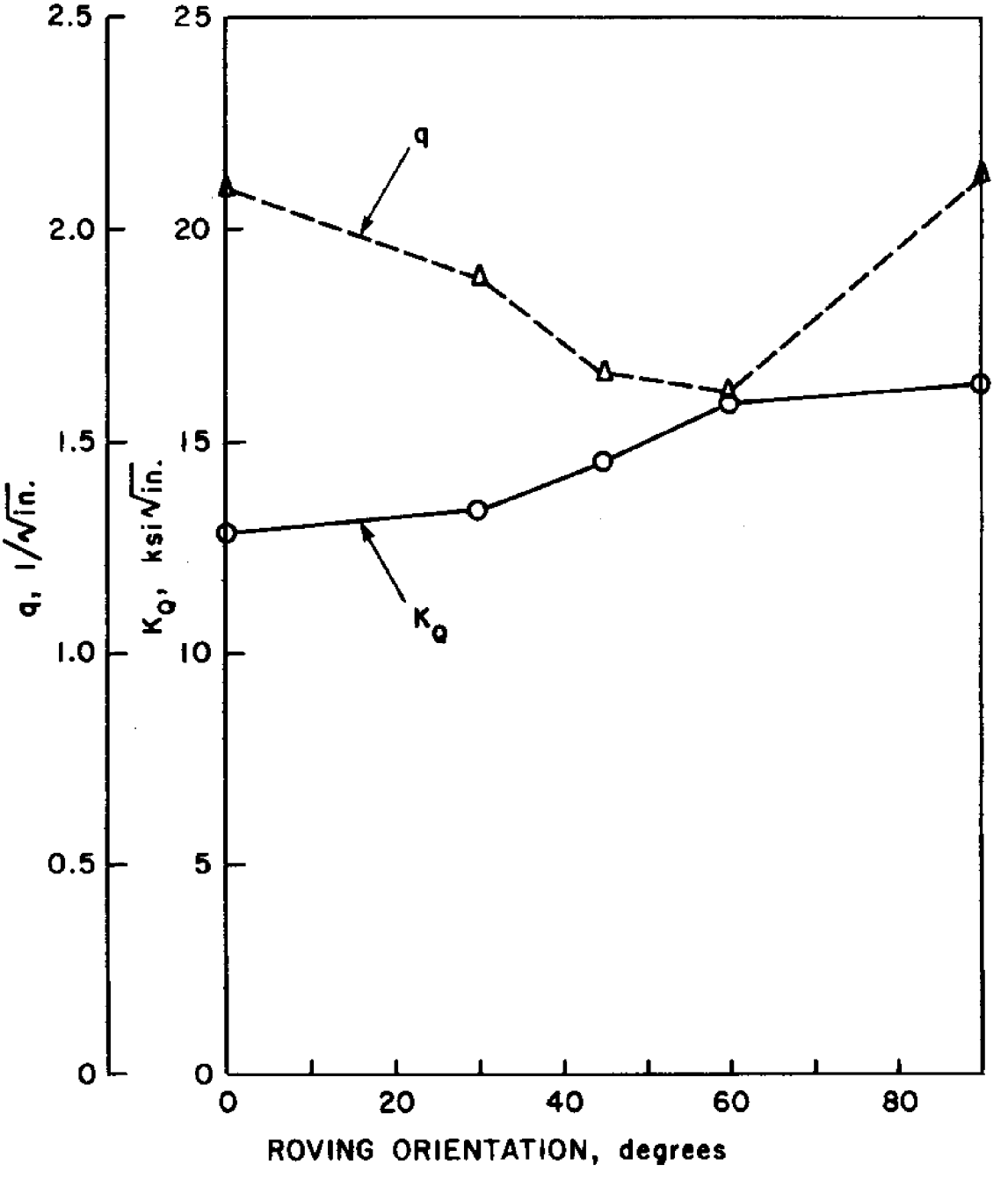

FIGURE 10.

VARIATION OF FRACTURE TOUGHNESS, K_Q, AND GENERALIZED STRESS CONCENTRATION PARAMETER, q, WITH ROVING ORIENTATION FOR ROVING/MAT/POLYESTER MATERIAL, DEN TEST, ALL SIZES.

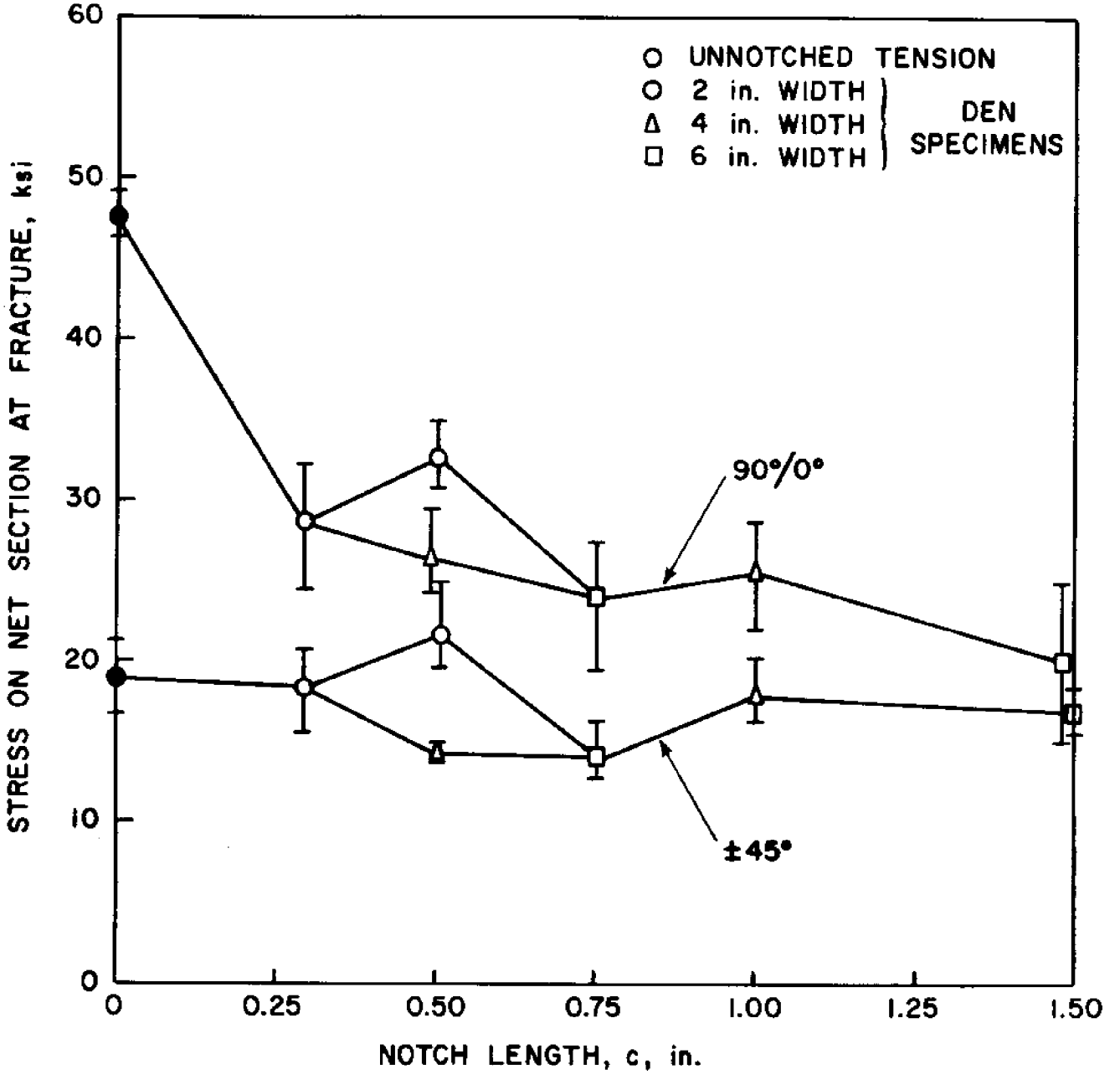

FIGURE 11.

VARIATION OF THE STRESS ON THE NET CROSS-SECTION BETWEEN NOTCHES AT FRACTURE WITH NOTCH LENGTH FOR 3 PLY 90° AND 45° WOVEN ROVING/POLYESTER, DEN TEST.

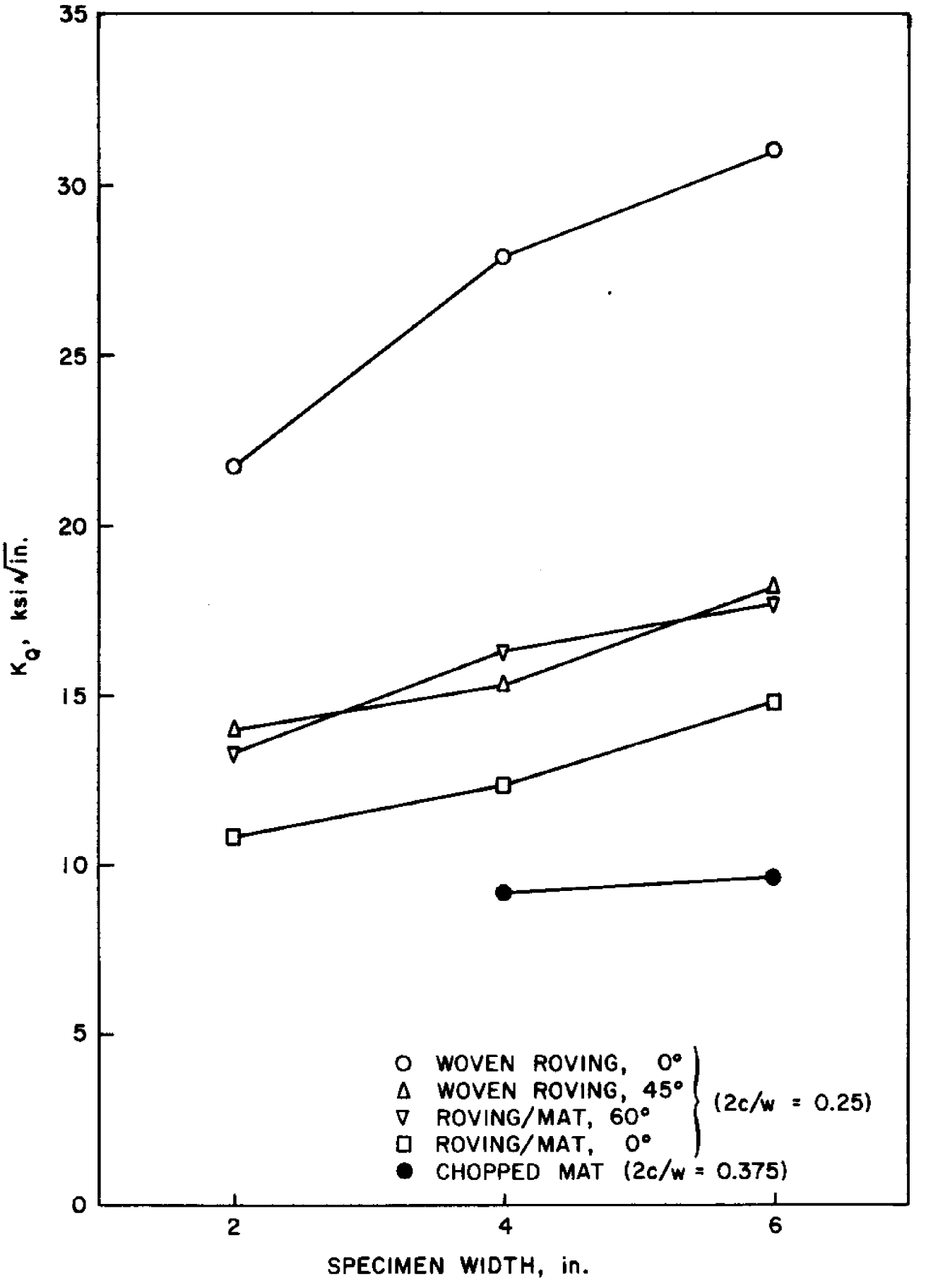

FIGURE 12.

FRACTURE TOUGHNESS vs. SPECIMEN WIDTH FOR VARIOUS MATERIALS, DEN TEST (2c/w = 0.25).

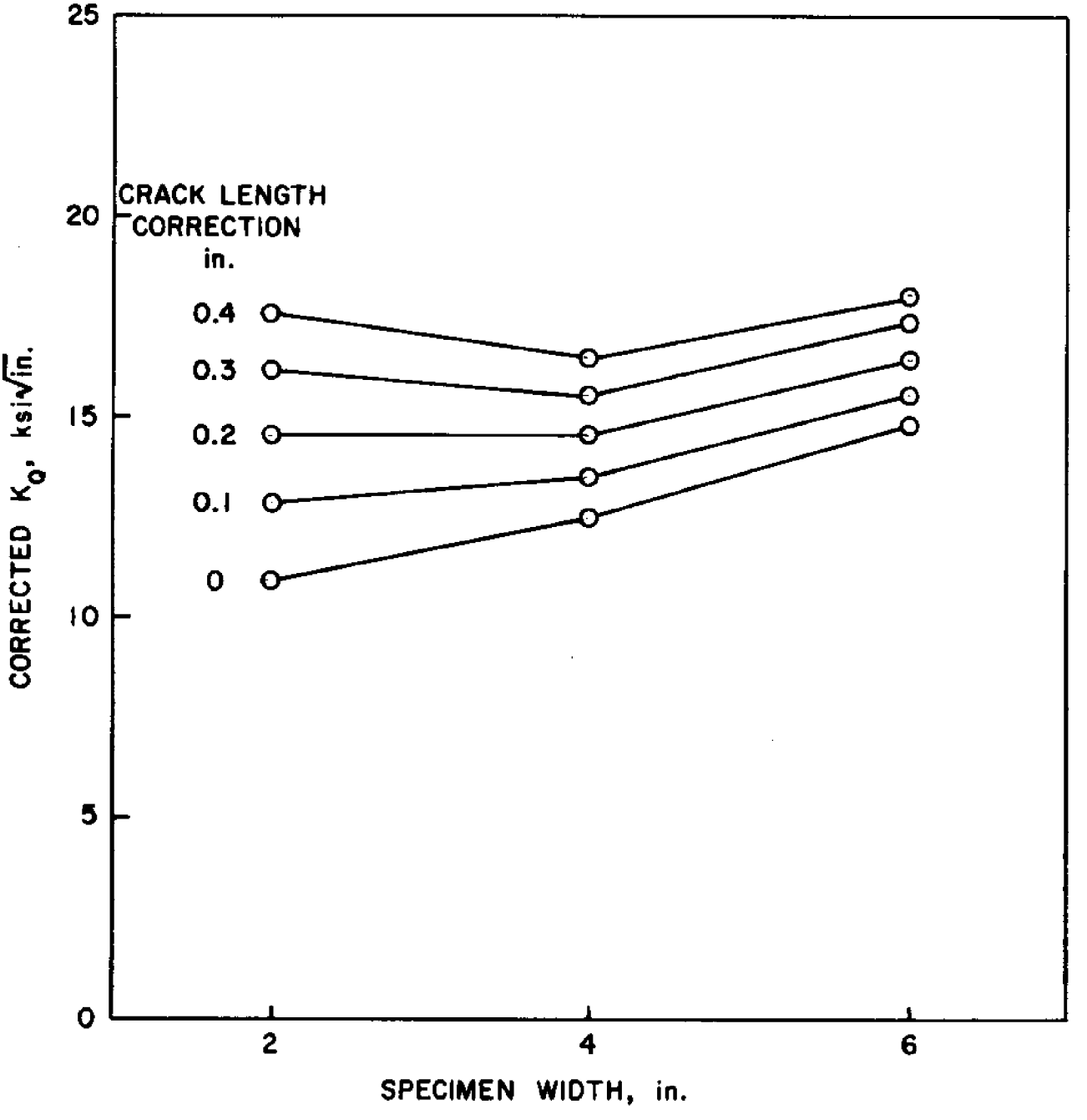

FIGURE 13.

CRACK LENGTH CORRECTION CURVES FOR FRACTURE TOUGHNESS OF ROVING/MAT/POLYESTER MATERIAL WITH 0° ROVING, DEN TEST (2c/w = 0.25).

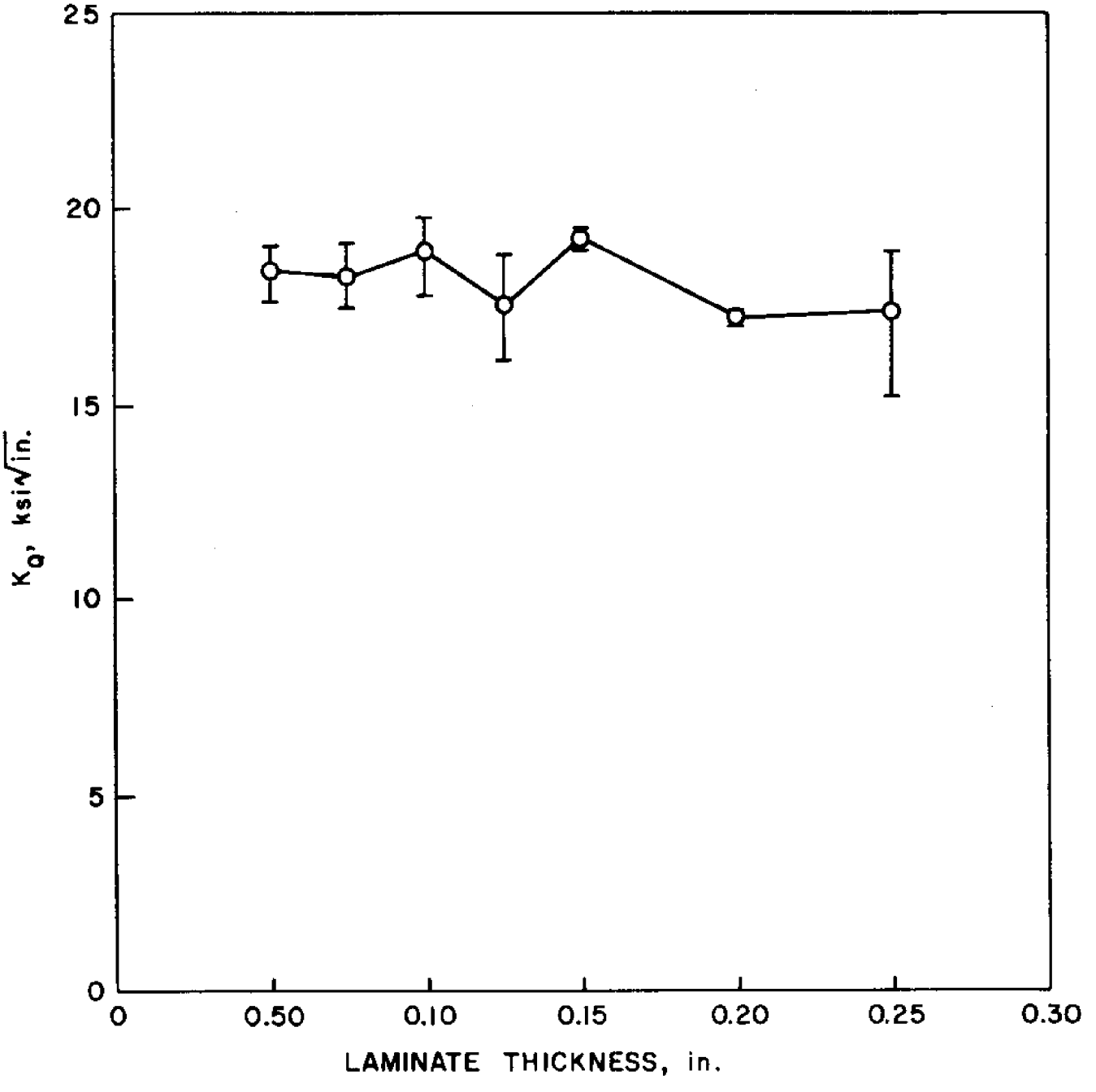

FIGURE 14.

FRACTURE TOUGHNESS vs. LAMINATE THICKNESS, 181 FABRIC/POLYESTER, DEN TEST (2c/w = 0.50).

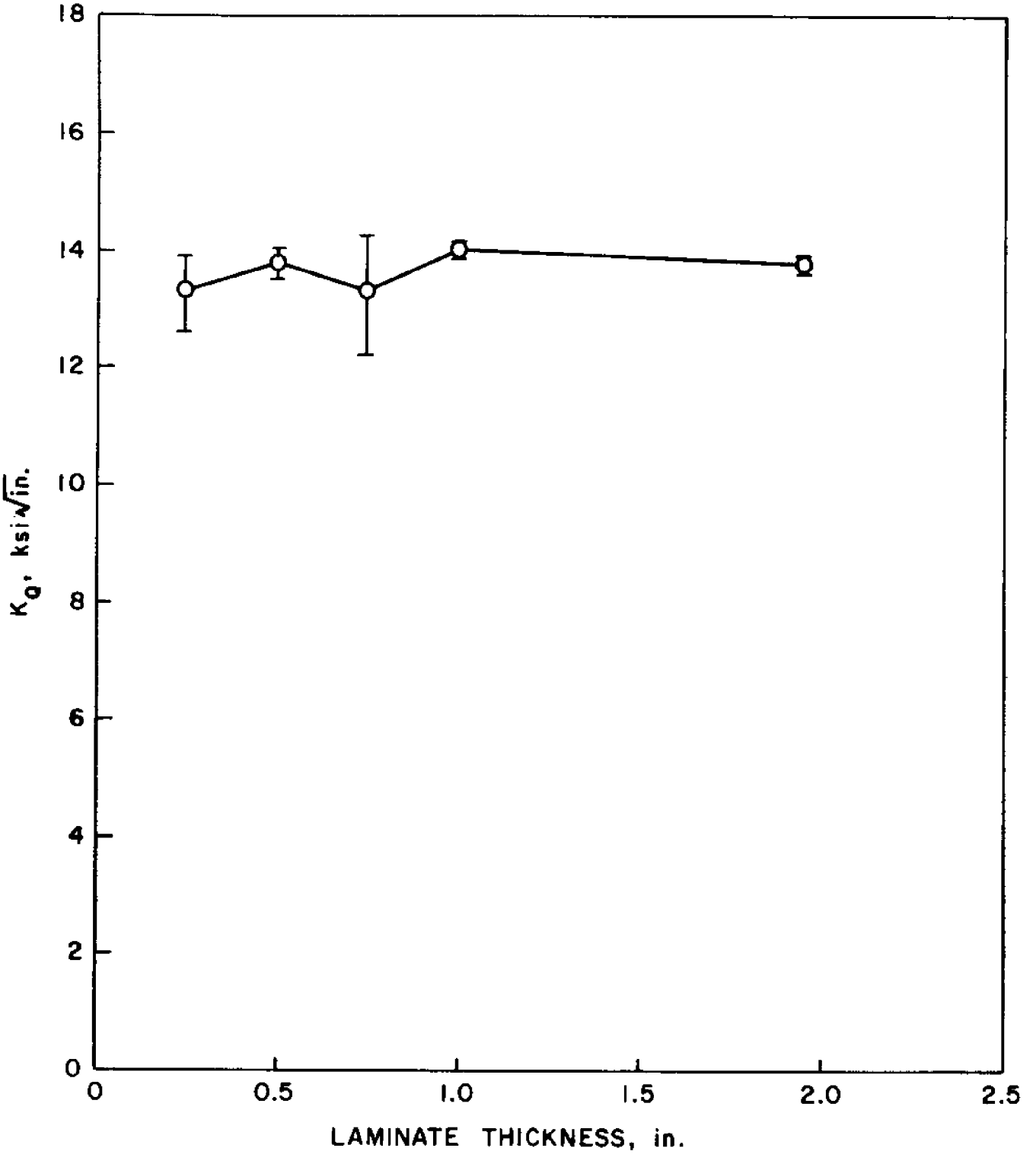

FIGURE 15.

FRACTURE TOUGHNESS vs. LAMINATE THICKNESS, ROVING/MAT/ POLYESTER MATERIAL WITH 0° ROVING, CLEAVAGE TEST.

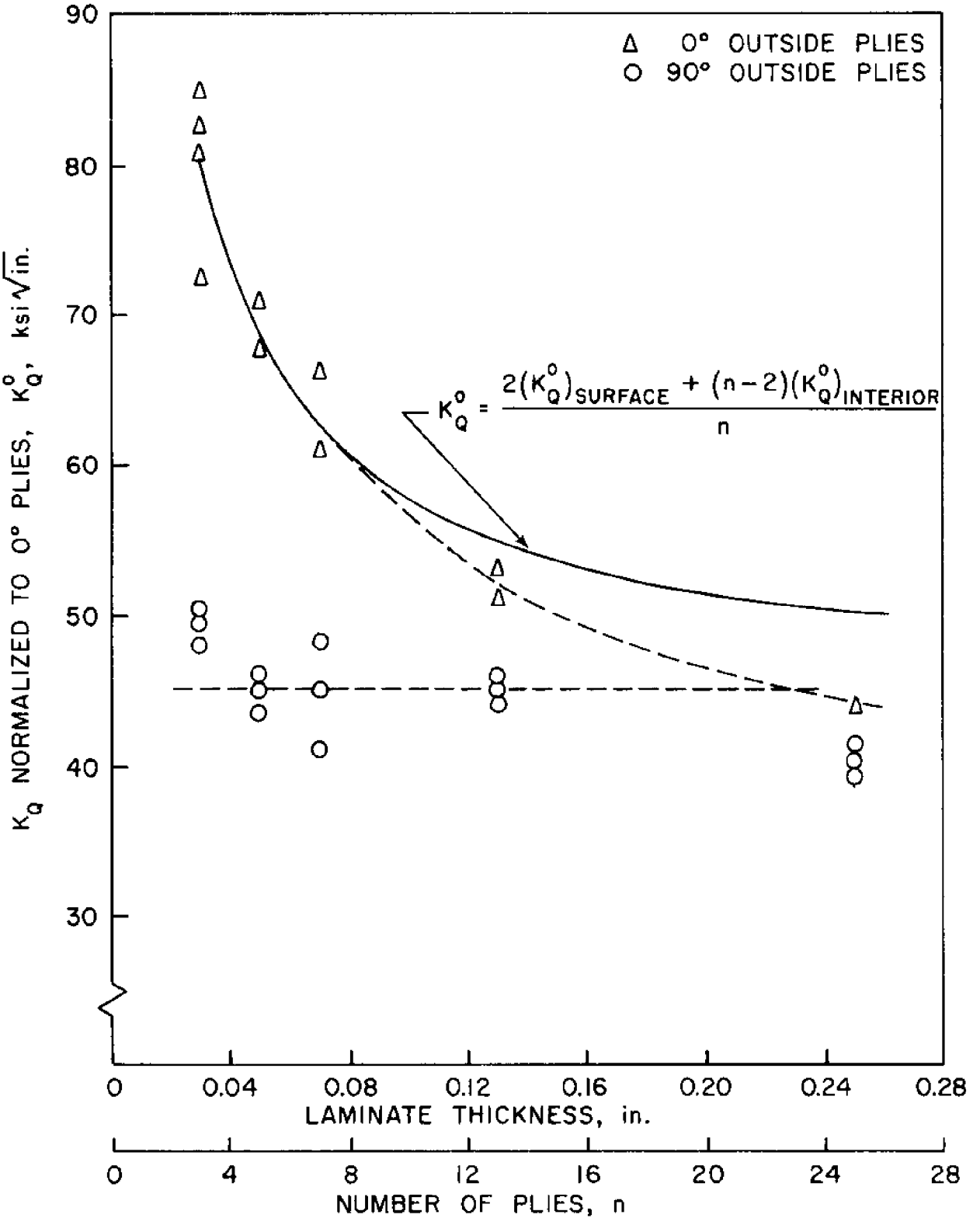

FIGURE 16.

FRACTURE TOUCHNESS vs. LAMINATE THICKNESS FOR 90/0/90/0/. . . ./90 AND 0/90/0/90/. . . ./0 SCOTCHPLY GLASS/EPOXY LAMINATES, DEN TEST (2c/w = 0.25).

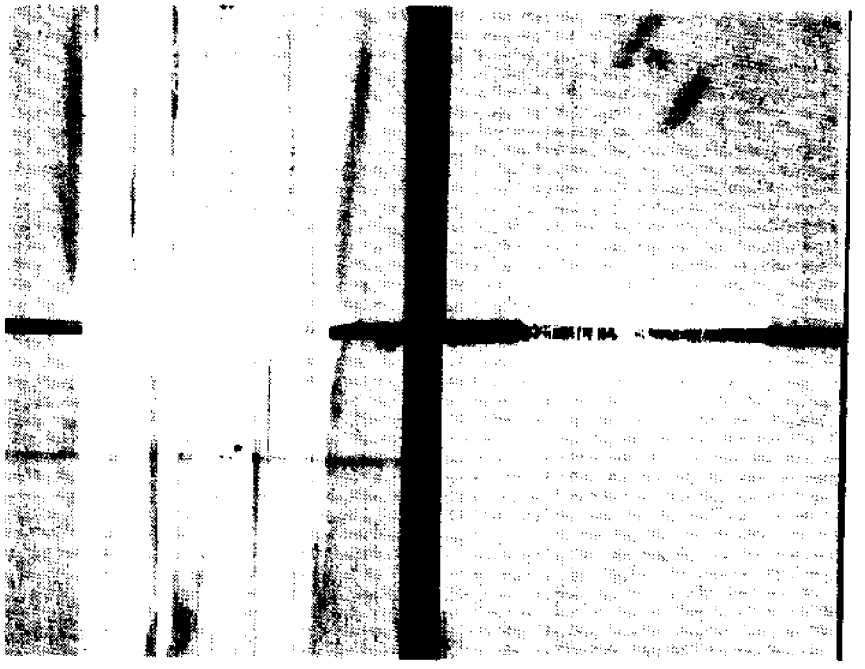

FIGURE 17.

FRACTURED SPECIMENS OF 90/0/90/0/. . . ./90 (RIGHT) AND 0/90/0/90/. . . ./0 (LEFT) SCOTCHPLY GLASS/EPOXY LAMINATE.

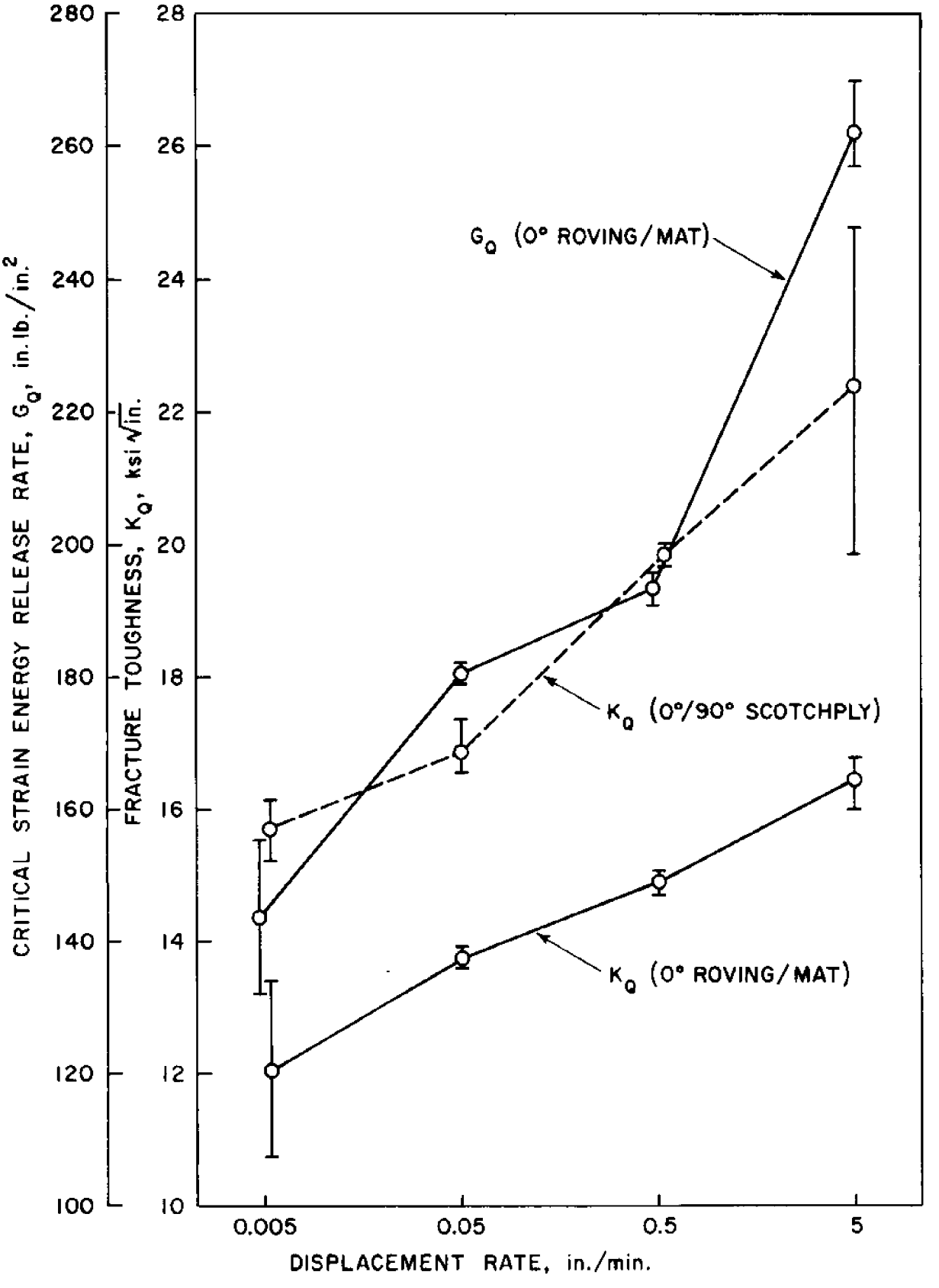

FIGURE 18.

EFFECT OF DISPLACEMENT RATE ON FRACTURE TOUGHNESS AND CRITICAL STRAIN ENERGY RELEASE RATE FOR 0° ROVING/MAT/POLYESTER (CLEAVAGE TEST), AND (90/0/90/0/90) SCOTCHPLY (DEN TEST), AT 75°F.

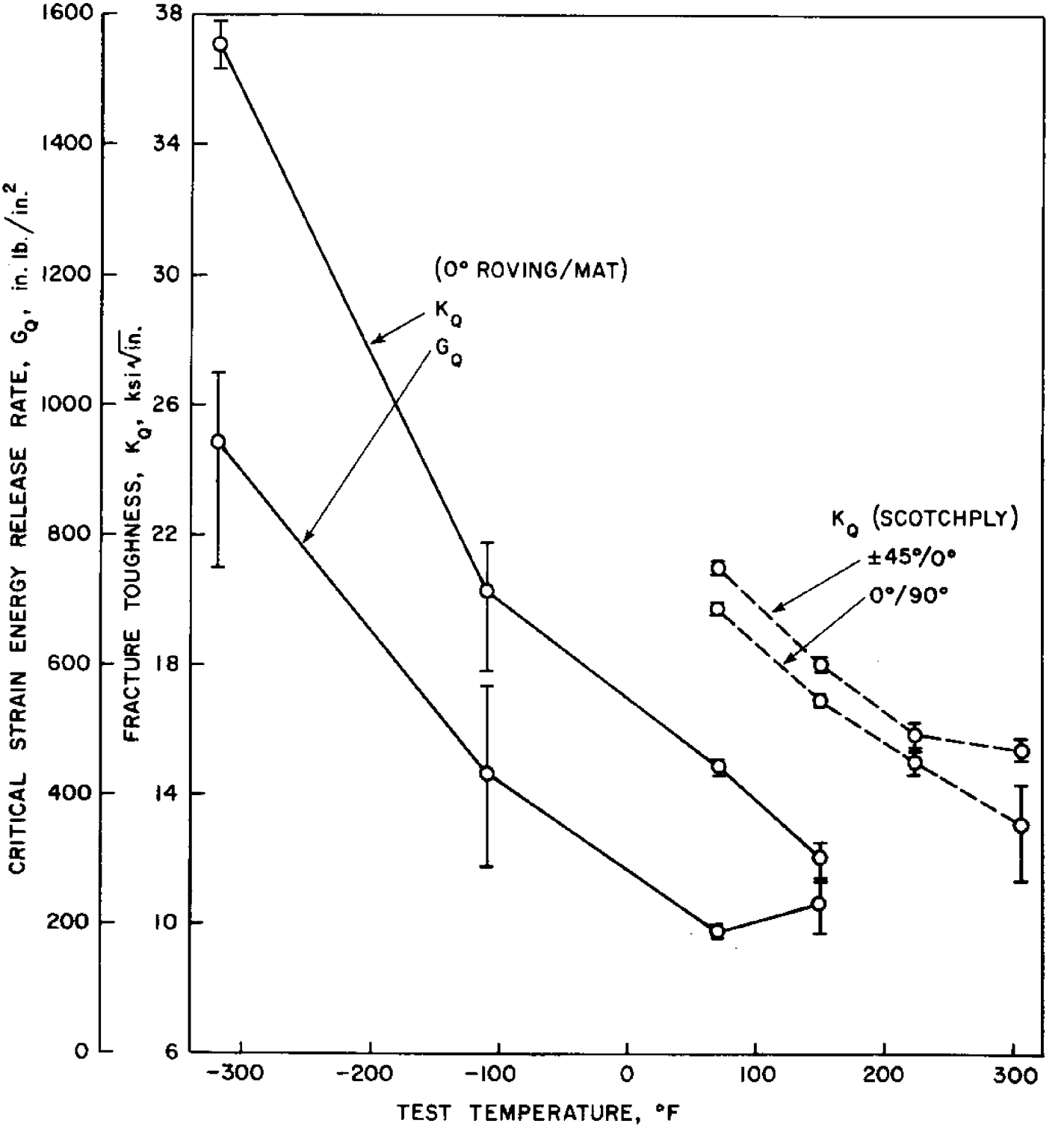

FIGURE 19.

EFFECT OF TEST TEMPERATURE ON FRACTURE TOUGHNESS AND CRITICAL STRAIN ENERGY RELEASE RATE FOR 0° ROVING/MAT/POLYESTER (CLEAVAGE TEST), AND (90/0/90/0/90) AND (45/-45/0/-45/45) SCOTCHPLY (DEN TEST), AT 0.5 in./min. DISPLACEMENT RATE.